Appendix G

Appendix G-1

EPA 2016v2 Emissions Platform TSD

Air Quality Modeling for the 2016v2 Emissions Platform Technical Support Document

Office of Air Quality Planning and Standards
United States Environmental Protection
Agency January 2022

Note: EPA originally posted this document on January 18, 2022. This document, posted on January 19, 2022, corrects an inadvertent error. The revised language is indicated in red font at the bottom of page A-11.

1. Introduction

In this technical support document (TSD) we describe the air quality modeling performed using emissions from the 2016v2. The focus of the air quality modeling is to project ozone design values[1] at individual monitoring sites to 2023, 2026, and 2032 and to estimate state-by-state contributions to ozone design values at individual monitoring sites in 2023 and 2026.

In brief, EPA performed air quality modeling for a 2016 base year and 2023, 2026, and 2032 future years to project 2016-centered base period design values to each of these future years. Ozone source apportionment modeling was performed using emissions in 2023 and 2026 to determine the contributions of total anthropogenic emissions in each state to projected ozone design values at individual monitoring sites nationwide for each of these years.

The remaining sections of this TSD are as follows. Section 2 describes the air quality modeling platform and the evaluation of model predictions using measured concentrations. Section 3 defines the procedures for projecting ozone design value concentrations and Section 4 describes (1) the source apportionment modeling and (2) the procedures for calculating the average contribution metric. For questions about the information in this TSD and to request a copy of the model input and/or output files please contact Norm Possiel at possiel.norm@epa.gov.

2. Air Quality Modeling Platform

The EPA used a 2016-based air quality modeling platform to provide the foundational model-input data sets for 2016 and the future analytic years. These inputs include emissions for 2016, 2023, 2026, and 2032 developed using the 2016v2 emissions modeling platform as well as meteorology, initial and boundary condition concentrations and other inputs representative of the 2016 base year. The 2016 v2 emissions modeling platform is described in the document *Preparation of Emissions Inventories for the 2016v2 North American Emissions Modeling Platform*. https://www.epa.gov/air-emissions-modeling/2016v2-platform. The meteorological and initial and boundary condition files for air quality modeling and the model performance results are described below.

[1] The ozone design value for a monitoring site is the 3-year average of the annual fourth-highest daily maximum 8-hour average ozone concentrations at the site.

2.1 Air Quality Model Configuration and Model Simulations

The photochemical model simulations used the Comprehensive Air Quality Model with Extensions (CAMx version 7.10).[2] CAMx is a three-dimensional grid-based Eulerian air quality model designed to simulate the formation and fate of oxidant precursors, primary and secondary particulate matter concentrations, and deposition over regional and urban spatial scales (e.g., the contiguous U.S.). Consideration of the different processes (e.g., transport and deposition) that affect primary (directly emitted) and secondary (formed by atmospheric processes) pollutants at the regional scale in different locations is fundamental to understanding and assessing the effects of emissions on air quality concentrations. EPA used the CAMx Ozone Source Apportionment Technology/Anthropogenic Precursor Culpability Analysis (OSAT/APCA) technique[3] to model ozone contributions, as described below in Section 4.

The geographic extent of the modeling domains that were used for air quality modeling in this analysis are shown in Figure 2-1. The large domain covers the 48 contiguous states along with most of Canada and all of Mexico with a horizontal resolution of 36 x 36 km. Air quality modeling for the 36 km domain was used to provide boundary conditions for the nested 12 km x 12 km domain air quality model runs. Both modeling domains have 25 vertical layers with a top at about 17,550 meters, or 50 millibars (mb). The model simulations produce hourly air quality concentrations for each grid cell across each modeling domain.

[2] Ramboll Environment and Health, January 2021, http://www.camx.com.

[3] As part of this technique, ozone formed from reactions between biogenic VOC and NOx with anthropogenic NOx and VOC are assigned to the anthropogenic emissions.

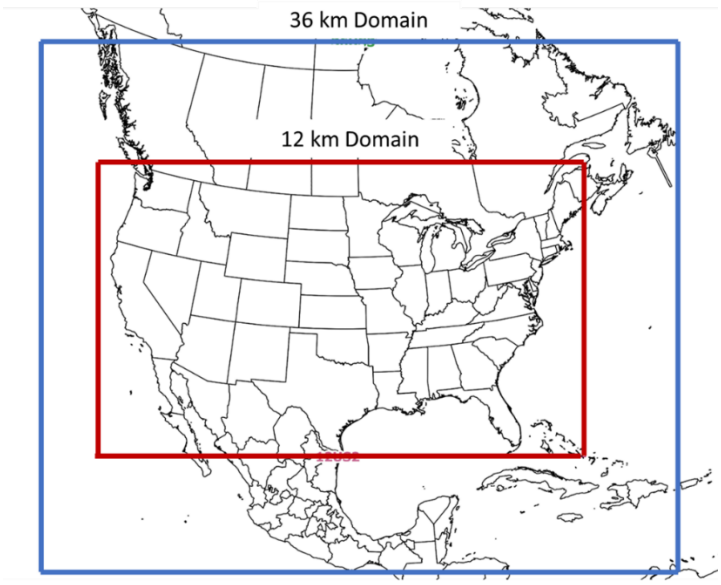

CAMx requires a variety of input files that contain information pertaining to the modeling domain and simulation period. These include gridded, hourly emissions estimates and meteorological data, and initial and boundary concentrations. Separate emissions inventories were prepared for the 2016 base year and the 2023, 2026, and 2032 projections. All other inputs (i.e. meteorological fields, initial concentrations, ozone column, photolysis rates, and boundary concentrations) were specified for the 2016 base year model application and remained unchanged for the projection-year model simulations.[4] The simulation period for each run was preceded by a 15-day ramp-up period.[5]

[4] EPA used the CAMx7.1chemparam.CB6r5_CF2E chemical parameter file for all the CAMx model runs described in this TSD.

[5] Note that the 2026fj case was run for January through April and October through December and the model concentration output were then combined with those from the 2026fj_ussa case to create outputs for an annual simulation.

2.2 Meteorological Data for 2016

This section describes the meteorological modeling that was performed to provide meteorological data for 2016 for input to air quality modeling. Note that EPA used the same meteorological data for the 2016v2 air quality modeling as was used for the 2016v1 air quality modeling.

The 2016 meteorological data were derived from running Version 3.8 of the Weather Research Forecasting Model (WRF) (Skamarock, et al., 2008). The meteorological outputs from WRF include hourly-varying horizontal wind components (i.e., speed and direction), temperature, moisture, vertical diffusion rates, and rainfall rates for each grid cell in each vertical layer. Selected physics options used in the WRF simulations include Pleim-Xiu land surface model (Xiu and Pleim, 2001; Pleim and Xiu, 2003), Asymmetric Convective Model version 2 planetary boundary layer scheme (Pleim 2007a,b), Kain-Fritsch cumulus parameterization (Kain, 2004) utilizing the moisture-advection trigger (Ma and Tan, 2009), Morrison double moment microphysics (Morrison, et al., 2005; Morrison and Gettelman, 2008), and RRTMG longwave and shortwave radiation schemes (Iacono, et.al., 2008).

Both the 36 km and 12 km WRF model simulations utilize a Lambert conformal projection centered at (-97,40) with true latitudes of 33 and 45 degrees north. The 36 km domain contains 184 cells in the X direction and 160 cells in the Y direction. The 12 km domain contains 412 cells in the X direction and 372 cells in the Y direction. The atmosphere is resolved with 35 vertical layers up to 50 mb (see Table 2-1), with the thinnest layers being nearest the surface to better resolve the planetary boundary layer (PBL).

The 36 km WRF model simulation was initialized using the 0.25-degree GFS analysis and 3-hour forecast from the 00Z, 06Z, 12Z, and 18Z simulations. The 12 km model was initialized using the 12km North American Model (12NAM) analysis product provided by National Climatic Data Center (NCDC).[6] The 40km Eta Data Assimilation System (EDAS) analysis (ds609.2) from the National Center for Atmospheric Research (NCAR) was used where 12NAM data was unavailable.[7] Analysis nudging for temperature, wind, and moisture was applied above the boundary layer only. The model simulations were conducted continuously.

[6] https://www.ncdc.noaa.gov/data-access/model-data/model-datasets/north-american-mesoscale-forecast-system-nam

[7] https://www.ready.noaa.gov/edas40.php.

The ‘ipxwrf’ program was used to initialize deep soil moisture at the start of the run using a 10-day spinup period (Gilliam and Pleim, 2010). Landuse and land cover data were based on the USGS for the 36NOAM simulation and the 2011 National Land Cover Database (NLCD 2011) for the 12US simulation. Sea surface temperatures were ingested from the Group for High Resolution Sea Surface Temperatures (GHRSST) (Stammer et al., 2003) 1 km SST data.

Additionally, lightning data assimilation was utilized to suppress (force) deep convection where lightning is absent (present) in observational data. This method is described by Heath et al. (2016) and was employed to help improve precipitation estimates generated by the model.

Table 2-1. Vertical layers and their approximate height above ground level.

WRF Layer	Height (m)	Pressure (mb)	Sigma
35	17,556	5000	0.000
34	14,780	9750	0.050
33	12,822	14500	0.100
32	11,282	19250	0.150
31	10,002	24000	0.200
30	8,901	28750	0.250
29	7,932	33500	0.300
28	7,064	38250	0.350
27	6,275	43000	0.400
26	5,553	47750	0.450
25	4,885	52500	0.500
24	4,264	57250	0.550
23	3,683	62000	0.600
22	3,136	66750	0.650
21	2,619	71500	0.700
20	2,226	75300	0.740
19	1,941	78150	0.770
18	1,665	81000	0.800
17	1,485	82900	0.820
16	1,308	84800	0.840
15	1,134	86700	0.860
14	964	88600	0.880
13	797	90500	0.900
12	714	91450	0.910
11	632	92400	0.920
10	551	93350	0.930
9	470	94300	0.940
8	390	95250	0.950
7	311	96200	0.960
6	232	97150	0.970
5	154	98100	0.980
4	115	98575	0.985

WRF Layer	Height (m)	Pressure (mb)	Sigma
3	77	99050	0.990
2	38	99525	0.995
1	19	99763	0.9975
Surface	0	100000	1.000

The meteorological data generated by the WRF simulations were processed using wrfcamx v4.7 (Ramboll 2021) meteorological data processing program to create model-ready meteorological inputs to CAMx. In running wrfcamx, vertical eddy diffusivities (Kv) were calculated using the Yonsei University (YSU) (Hong and Dudhia, 2006) mixing scheme. We used a minimum Kv of 0.1 m^2/sec except for urban grid cells where the minimum Kv was reset to 1.0 m^2/sec within the lowest 200 m of the surface in order to enhance mixing associated with the nighttime "urban heat island" effect. In addition, we invoked the subgrid convection and subgrid stratoform cloud options in our wrfcamx run for 2016.

2.3 Initial and Boundary Concentrations

The lateral boundary and initial species concentrations for the 36 km modeling domain are provided by a three-dimensional global atmospheric chemistry model, the Hemispheric version of the Community Multi-scale Air Quality Model (H-CMAQ) version 3.1.1. The H-CMAQ predictions were used to provide one-way dynamic boundary concentrations at one-hour intervals and an initial concentration field for the 36 km CAMx simulations. The air quality predictions from the 36 km CAMx simulation for 2016 were used to provide boundary concentrations for the 12 km 2016 modeling. In addition to providing initial and boundary concentrations for the 12 km 2023 model run, the predictions from the 2023 36 km model run were also used to provide boundary conditions for the 12 km modeling for 2026 and 2032. More information about the H-CMAQ model and other applications using this tool is available at: https://www.epa.gov/cmaq/hemispheric-scale-applications. Note that EPA used the same initial and boundary conditions for the 2016v2 air quality modeling as was used for the 2016v1 air quality modeling.

2.5 Air Quality Model Evaluation

An operational model performance evaluation for ozone was conducted to examine the ability of the CAMx modeling system to simulate 2016 measured concentrations. This evaluation focused on graphical analyses and statistical metrics of model predictions versus observations. Details on the evaluation methodology, the calculation of performance statistics, and results are provided in Appendix A. Overall, the ozone model performance statistics for the CAMx 2016 simulation are within or close to the ranges found in other recent peer-reviewed applications (e.g., Simon et al, 2012 and Emory et al, 2017). As described in Appendix A, the predictions from the 2016v2 modeling platform correspond closely to observed concentrations in terms of the magnitude, temporal fluctuations, and geographic differences for 8-hour daily maximum (MDA8) ozone. Thus, the model performance results demonstrate the scientific credibility of our 2016v2 modeling platform. These results provide confidence in the ability of the modeling platform to provide a reasonable projection of expected future year ozone concentrations and contributions.

3. Approach for Projecting Ozone Design Values

The ozone predictions from the CAMx model simulations were used to project ambient (i.e., measured) ozone design values (DVs) to 2023, 2026, and 2032 based on an approach that follows from EPA's guidance for attainment demonstration modeling (US EPA, 2018),[8] as summarized here. The modeling guidance recommends using 5-year weighted average ambient design values centered on the base modeling year as the starting point for projecting average design values to the future. Because 2016 is the base emissions year, we used the average ambient 8-hour ozone design values for the period 2014 through 2018 (i.e., the average of design values for 2014-2016, 2015-2017 and 2016-2018) to calculate the 5-year weighted average design values (i.e., 2016-Centered design values). The 5-year weighted average ambient design value at each site was projected to 2023, 2026, and 2032 using the Software for Model Attainment Test Software – Community Edition (SMAT-CE). This program calculates the 5-year weighted average design value based on observed data and projects future year values using the

[8] EPA's ozone attainment demonstration modeling guidance is referred to as "the modeling guidance" in the remainder of this document.

relative response predicted by the model. Equation (3-1) describes the recommended model attainment test in its simplest form, as applied for monitoring site *i*:

$$(\mathrm{DVF})_i = (RRF)_i * (DVB)_i \qquad \text{Equation 3-1}$$

$\mathrm{DVF_i}$ is the estimated design value for the future year at monitoring site *i*; $\mathrm{RRF_i}$ is the relative response factor for monitoring site *i*; and $\mathrm{DVB_i}$ is the base period design value monitored at site *i*. The relative response factor for each monitoring site $(RRF)_i$ is the fractional change in MDA8 ozone between the base and future year. The RRF is based on the average ozone on model-predicted "high" ozone days in grid cells in the vicinity of the monitoring site. The modeling guidance recommends calculating RRFs based on the highest 10 modeled ozone days in the base year simulation at each monitoring site. Specifically, the RRF was calculated based on the 10 highest days in the 2016 base year modeling in the vicinity of each monitor location. For cases in which the base year model simulation did not have 10 days with ozone values greater than or equal to 60 ppb at a site, we used all days with ozone >= 60 ppb, as long as there were at least 5 days that meet that criteria. At monitor locations with less than 5 days with modeled 2016 base year ozone >= 60 ppb, no RRF or DVF was calculated for the site and the monitor in question was not included in this analysis.

The modeling guidance recommends calculating the RRF using the base year and future year model predictions from the cells immediately surrounding the monitoring site along with the grid cell in which the monitor is located. In this approach the RRF was based on a 3 x 3 array of 12 km grid cells centered on the location of the grid cell containing the monitor.

The EPA also projected design values based on a modified version of the "3 x 3" approach for those monitoring sites located in coastal areas. In this alternative approach, EPA eliminated from the RRF calculations the modeling data in those grid cells that are dominated by water (i.e., more than 50 percent of the area in the grid cell is water) and that do not contain a monitoring site (i.e., if a grid cell is more than 50 percent water but contains an air quality monitor, that cell would remain in the calculation). The choice of more than 50 percent of the grid cell area as water as the criteria for identifying overwater grid cells is based on the treatment of land use in the Weather Research and Forecasting model (WRF).[9] Specifically, in the WRF meteorological model those grid cells that are greater than 50 percent overwater are

[9] https://www.mmm.ucar.edu/weather-research-and-forecasting-model.

treated as being 100 percent overwater. In such cases the meteorological conditions in the entire grid cell reflect the vertical mixing and winds over water, even if part of the grid cell also happens to be over land with land-based emissions, as can often be the case for coastal areas. Overlaying land-based emissions with overwater meteorology may be representative of conditions at coastal monitors during times of on-shore flow associated with synoptic conditions and/or sea-breeze or lake-breeze wind flows. But there may be other times, particularly with off-shore wind flow when vertical mixing of land-based emissions may be too limited due to the presence of overwater meteorology. Thus, for the 2016v2 modeling EPA calculated projected average and maximum design values at individual monitoring sites based on both the "3 x 3" approach as well as the alternative approach that eliminates overwater cells in the RRF calculation for near-coastal areas (i.e., "no water" approach).

For both the "3 x 3" approach and the "no water" approach, the grid cell with the highest base year MDA8 ozone concentration on each day in the applicable array of grid cells surrounding the location of the monitoring site[10] is used for both the base and future components of the RRF calculation. That is, the base and future year data are paired in space for the grid cell that has the highest MDA8 concentration on the given day.

The approach for calculating projected maximum design values is similar to the approach for calculating the projected average design values. To calculate projected maximum design values we start with the highest (i.e., maximum) ambient design value from the 2016-Centered 5-year period (i.e., the maximum of design values from 2014-2016, 2014-2017, and 2016-2018). The base period maximum design value at each site was projected to 2023, 2026, and 2032 using the site-specific RRFs, as determined using the procedures for calculating RRFs described above. Consistent with the truncation and rounding procedures for the 8-hour ozone NAAQS, the projected design values are truncated to integers in units of ppb.[11] . Projected design values for 2023, 2026, and 2032 based on both the "3 x 3" and "no water" methods for individual monitoring sites nationwide are provided in the file "2016v2_DVs_state_contributions".

[10] For the "3 x 3" approach the applicable array contains the 9 grid cells that surround and include the grid cell containing the monitoring site. The applicable array for the "no water" approach includes the grid cell containing the monitoring site along with the subset of the "3 x 3" grid cells that are not classified as "water" grid cells using the criteria described in this TSD.

[11] 40 CFR Part 50, Appendix P to Part 50 – Interpretation of the Primary and Secondary National Ambient Air Quality Standards for Ozone.

4. Ozone Contribution Modeling

As noted above, EPA performed nationwide, state-level ozone source apportionment modeling using the CAMx OSAT/APCA technique to provide data on the contribution of projected 2023 and 2026 base case NO_X and VOC emissions from all anthropogenic source sectors combined, in each state. The state-by-state source apportionment modeling is described in section 4.1 and the method for calculating the average contribution metric for each source apportionment model run is described in section 4.2.

4.1 State-by-State Modeling

In the state-by-state source apportionment model run, we tracked the ozone formed from each of the following contribution categories (i.e., "tags"):

- States – anthropogenic NO_X and VOC emissions from each of the contiguous 48 states and the District of Columbia tracked individually (emissions from all anthropogenic sectors in a given state were combined);
- Biogenics – biogenic NO_X and VOC emissions domain-wide (i.e., not by state);
- Initial and Boundary Concentrations – air quality concentrations used to initialize the 12 km model simulation and air quality concentrations transported into the 12 km modeling domain from the lateral boundaries;
- Tribal – the emissions from those tribal lands for which we have point source inventory data in the 2016 emissions platform (we did not model the contributions from individual tribes);
- Canada and Mexico – anthropogenic emissions from sources in the portions of Canada and Mexico included in the 12 km modeling domain (contributions from Canada and Mexico were not modeled separately);
- Fires – combined emissions from wild and prescribed fires domain-wide within the 12 km modeling domain (i.e., not by state); and
- Offshore – combined emissions from offshore marine vessels and offshore drilling platforms (i.e., not by state).

The source apportionment modeling provided hourly contributions to ozone from anthropogenic NO_X and VOC emissions in each state, individually to ozone concentrations in each model grid cell. The contributions to ozone from chemical reactions between biogenic NO_X

and VOC emissions were modeled and assigned to the "biogenic" category. The contributions from wildfire and prescribed fire NO_X and VOC emissions were modeled and assigned to the "fires" category. The contributions from the "biogenic", "offshore", and "fires" categories are not assigned to individual states nor are they included in the state contributions.

4.2 Method for Calculating the Contribution Metric

As noted above, the state-by-state source apportionment model runs for 2023 and 2026 were performed for the period May 1 through October 1 using the projected 2023 and 2026 base case emissions and 2016 meteorology. The hourly contributions[12] from each tag were processed to calculate an 8-hour average contribution metric value for each tag at each monitoring site. The contribution metric values at each individual monitoring site are calculated using model predictions for the grid cell containing the monitoring site. The process for calculating the average contribution metric uses the source apportionment outputs in a "relative sense" to apportion the projected average design value at each monitoring location into contributions from each individual tag. This process is similar in concept to the approach described above for using model predictions to calculate future year ozone design values.

The basic approach used to calculate the average contribution metric values for 2023 is described by the following steps:

(1) For the model grid cells containing an ozone monitoring site, calculate the 8-hour average contribution from each source tag to each monitoring site for the time period of the 8-hour daily maximum modeled (i.e., MDA8) concentration on each day;

(2) Average the MDA8 concentrations for each of the top 10 modeled ozone concentration days in 2023 and average the 8-hour contributions for each of these same days for each tag;

(3) Divide the 10-day average contribution for each tag by the corresponding 10-day average concentration to obtain a Relative Contribution Factor (RCF) for each tag for each monitoring site;

(4) Multiply the 2023 average design values by the corresponding RCF to produce the average contribution metric values at each monitoring site in 2023.

[12] Contributions from anthropogenic emissions under "NO_X-limited" and "VOC-limited" chemical regimes were combined to obtain the net contribution from NO_X and VOC anthropogenic emissions in each state.

The contribution metric values calculated from step 4 are truncated to two digits to the right of the decimal (e.g., a calculated contribution of 0.78963… is truncated to 0.78 ppb). As a result of truncation, the tabulated contributions may not always sum to the future year average design value.

To calculate contribution metric values for the 2026 source apportionment model runs, EPA followed the same approach as described above for 2023, except that we calculated the average contribution metric values for 2026 using the 2026 MDA8 concentrations and 2026 8-hour average contributions for the same dates that were used to calculate the contribution metric values in 2023. Even though 2026 is only 3 years beyond 2023, it is possible that changes in projected emissions between 2023 and 2026 could potentially result in a change in the ranking of model-predicted MDA8 ozone concentrations in 2026 compared to 2023 at some monitoring sites. Using modeled data for from the same set of dates when calculating contribution metric values for 2023 and 2026 provides for consistency in terms of the meteorology associated with the contribution values in 2023 and 2026. The contribution metric values for monitoring sites nationwide for the 2023 and 2026 state-by-state source apportionment model runs are provided in the file "2016v2_DVs_state_contributions".

5. References

Emery, C., Z. Liu, A. Russell, M. T. Odom, G. Yarwood, and N. Kumar, 2017. Recommendations on Statistics and Benchmarks to Assess Photochemical Model Performance. *J. Air and Waste Management Association*, 67, 582-598.

Gilliam, R.C. and J.E. Pleim, 2010. Performance Assessment of New Land Surface and Planetary Boundary Layer Physics in the WRF-ARW. *J. Appl. Meteor. Climatol.*, **49**, 760–774.

Henderson, B.H., F. Akhtar, H.O.T. Pye, S.L. Napelenok, W.T. Hutzell, 2014. A Database and Tool for Boundary Conditions for Regional Air Quality Modeling: Description and Evaluations, *Geoscientific Model Development*, **7**, 339-360.

Hong, S-Y, Y. Noh, and J. Dudhia, 2006. A New Vertical Diffusion Package with an Explicit Treatment of Entrainment Processes. *Mon. Wea. Rev.*, 134, 2318–2341.

Houyoux, M.R., Vukovich, J.M., Coats, C.J., Wheeler, N.J.M., Kasibhatla, P.S.,2000. Emissions Inventory Development and Processing for the Seasonal Model for Regional Air Quality (SMRAQ) project, *Journal of Geophysical Research – Atmospheres*, 105(D7), 9079-9090.

Iacono, M.J., J.S. Delamere, E.J. Mlawer, M.W. Shephard, S.A Clough, and W.D. Collins, 2008. Radiative Forcing by Long-Lived Greenhouse Gases: Calculations with the AER Radiative Transfer Models, *J. Geophys. Res.,* 113, D13103.

Kain, J.S., 2004. The Kain-Fritsch Convective Parameterization: An Update, *J. Appl. Meteor.,* 43, 170-181.

Ma, L-M. and Tan Z-M, 2009. Improving the Behavior of Cumulus Parameterization for Tropical Cyclone Prediction: Convective Trigger, *Atmospheric Research*, 92, 190-211.

Morrison, H.J., A. Curry, and V.I. Khvorostyanov, 2005. A New Double-Moment Microphysics Parameterization for Application in Cloud and Climate Models. Part I: Description, *J. Atmos. Sci.*, 62, 1665–1677.

Morrison, H. and A. Gettelman, 2008. A New Two-Moment Bulk Stratiform Cloud Microphysics Scheme in the Community Atmosphere Model, version 3 (CAM3). Part I: Description and Numerical Tests, *J. Climate,* 21, 3642-3659.

Pleim, J.E. and A. Xiu, 2003. Development of a Land-Surface Model. Part II: Data Assimilation, *J. Appl. Meteor.*, 42, 1811–1822

Pleim, J.E., 2007a. A Combined Local and Nonlocal Closure Model for the Atmospheric Boundary Layer. Part I: Model Description and Testing, *J. Appl. Meteor. Climatol.*, 46, 1383–1395.

Pleim, J.E., 2007b. A Combined Local and Nonlocal Closure Model for the Atmospheric Boundary Layer. Part II: Application and Evaluation in a Mesoscale Meteorological Model, *J. Appl. Meteor. Climatol.*, 46, 1396–1409.

Ramboll Environ, 2021. User's Guide Comprehensive Air Quality Model with Extensions version 7.1, www.camx.com. Ramboll Environ International Corporation, Novato, CA.

Skamarock, W.C., J.B. Klemp, J. Dudhia, et al., 2008. A Description of the Advanced Research WRF Version 3. NCAR Tech. Note NCAR/TN-475+STR. http://wwww.mmm.ucar.edu/wrf/users/docs/arw_v3.pdf

Simon, H., K.R. Baker, and S.B. Phillips, 2012. Compilation and Interpretation of Photochemical Model Performance Statistics Published between 2006 and 2012, *Atmospheric Environment*, 61, 124-139.

Stammer, D., F.J. Wentz, and C.L. Gentemann, 2003. Validation of Microwave Sea Surface Temperature Measurements for Climate Purposes, *J. of Climate*, 16(1), 73-87.

U.S. Environmental Protection Agency, 2018. Modeling Guidance for Demonstrating Attainment of Air Quality Goals for Ozone, PM2.5, and Regional Haze, Research Triangle Park, NC. https://www3.epa.gov/ttn/scram/guidance/guide/O3-PM-RH-Modeling_Guidance-2018.pdf

Xiu, A., and J.E. Pleim, 2001, Development of a Land Surface Model. Part I: Application in a Meso scale Meteorological Model, *J. Appl. Meteor.,* 40, 192-209.

Yantosca, B. 2004. GEOS-CHEMv7-01-02 User's Guide, Atmospheric Chemistry Modeling Group, Harvard University, Cambridge, MA.

Appendix A

Model Performance Evaluation for 2016v2 Base Year CAMx Simulation

An operational model evaluation was conducted for the 2016 base year CAMx v7.1 simulation performed for the 12 km U.S. modeling domain. The purpose of this evaluation is to examine the ability of the 2016 air quality modeling platform to represent the magnitude and spatial and temporal variability of measured (i.e., observed) ozone concentrations within the modeling domain. The evaluation presented here is based on model simulations using the 20162 emissions platform (i.e., scenario name 2016fj). The model evaluation for ozone focuses on comparisons of model predicted 8-hour daily maximum concentrations to the corresponding observed data at monitoring sites in the EPA Air Quality System (AQS). The locations of the ozone monitoring sites in this network are shown in Figure A-1.

This evaluation includes statistical measures and graphical displays of model performance based upon model-predicted versus observed concentrations. In general, the evaluation focusses on model predicted and observed maximum daily average 8-hour (MDA8) ozone concentrations that were paired in space and time for the period May through September. Model performance statistics were calculated for several spatial scales and temporal periods. Statistics were calculated for individual monitoring sites and in aggregate for monitoring sites within each of nine climate regions of the 12 km U.S. modeling domain. The regions include the Northeast, Ohio Valley, Upper Midwest, Southeast, South, Southwest, Northern Rockies,

Northwest and West[13,14], which are defined based upon the states contained within the National Oceanic and Atmospheric Administration (NOAA) climate regions (Figure A-2).[15]

In addition to performance statistics, we prepared several graphical presentations of model performance for MDA8 ozone. These graphical presentations include:
(1) maps that show the mean bias and error as well as normalized mean bias and error calculated for MDA8 ≥ 60 ppb for May through September at individual monitoring sites;
(2) bar and whisker plots that show the distribution of the predicted and observed MDA8 ozone concentrations by month (May through September) and by region; and
(3) time series plots (May through September) of observed and predicted MDA8 ozone concentrations for selected monitoring sites.

The Atmospheric Model Evaluation Tool (AMET) was used to calculate the model performance statistics used in this document (Gilliam et al., 2005). For this evaluation we have selected the mean bias, mean error, normalized mean bias, and normalized mean error to characterize model performance, statistics which are consistent with the recommendations in Simon et al. (2012) and EPA's photochemical modeling guidance (U.S. EPA, 2018).

Mean bias (MB) is the average of the difference (predicted – observed) divided by the total number of replicates (n). Mean bias is given in units of ppb and is defined as:

MB = $\frac{1}{n}\sum_{1}^{n}(P - O)$, where P = predicted and O = observed concentrations

[13] The nine climate regions are defined by States where: Northeast includes CT, DE, ME, MA, MD, NH, NJ, NY, PA, RI, and VT; Ohio Valley includes IL, IN, KY, MO, OH, TN, and WV; Upper Midwest includes IA, MI, MN, and WI; Southeast includes AL, FL, GA, NC, SC, and VA; South includes AR, KS, LA, MS, OK, and TX; Southwest includes AZ, CO, NM, and UT; Northern Rockies includes MT, NE, ND, SD, WY; Northwest includes ID, OR, and WA; and West includes CA and NV.

[14] Note most monitoring sites in the West region are located in California (see Figures 2A-2a and 2A-2b), therefore the statistics for the West region will be mostly representative of model performance in California ozone.

[15] NOAA, National Centers for Environmental Information scientists have identified nine climatically consistent regions within the contiguous U.S., http://www.ncdc.noaa.gov/monitoring-references/maps/us-climate-regions.php.

Mean error (ME) calculates the absolute value of the difference (predicted - observed) divided by the total number of replicates (*n*). Mean error is given in units of ppb and is defined as:

$$\text{ME} = \frac{1}{n}\sum_1^n |P - O|$$

Normalized mean bias (NMB) is the average the difference (predicted - observed) over the sum of observed values. NMB is a useful model performance indicator because it avoids over inflating the observed range of values, especially at low concentrations. Normalized mean bias is given in percentage units and is defined as:

$$\text{NMB} = \frac{\sum_1^n (P-O)}{\sum_1^n (O)} * 100$$

Normalized mean error (NME) is the absolute value of the difference (predicted - observed) over the sum of observed values. Normalized mean error is given in percentage units and is defined as:

$$\text{NME} = \frac{\sum_1^n |P-O|}{\sum_1^n (O)} * 100$$

As described in more detail below, the model performance statistics indicate that the 8-hour daily maximum ozone concentrations predicted by the 2016 CAMx modeling platform closely reflect the corresponding 8-hour observed ozone concentrations in each region of the 12 km U.S. modeling domain. The acceptability of model performance was judged by considering the 2016 CAMx performance results in light of the range of performance found in recent regional ozone model applications (Emery et al., NRC, 2002; Phillips et al., 2007; Simon et al., 2012; U.S. EPA, 2005; U.S. EPA, 2009; U.S. EPA, 2010.[16] These other modeling studies

[16] Christopher Emery, Zhen Liu, Armistead G. Russell, M. Talat Odman, Greg Yarwood & Naresh Kumar (2017) Recommendations on statistics and benchmarks to assess photochemical model performance, Journal of the Air & Waste Management Association, 67:5, 582-598, DOI: 10.1080/10962247.2016.1265027
National Research Council (NRC), 2002. Estimating the Public Health Benefits of Proposed Air Pollution Regulations, Washington, DC: National Academies Press.
U.S. Environmental Protection Agency; Technical Support Document for the Final Clean Air Interstate Rule: Air Quality Modeling; Office of Air Quality Planning and Standards; RTP, NC; March 2005 (CAIR Docket OAR-2005-0053-2149).

represent a wide range of modeling analyses that cover various models, model configurations, domains, years and/or episodes, chemical mechanisms, and aerosol modules. Overall, the ozone model performance results for the 2016v2 CAMx simulation are within the range found in other recent peer-reviewed and regulatory applications. The model performance results, as described in this document, demonstrate that the predictions from the 2061v2 modeling platform correspond closely to observed concentrations in terms of the magnitude, temporal fluctuations, and geographic differences for 8-hour daily maximum ozone.

The 8-hour ozone model performance bias and error statistics for the period May-September for each region are provided in Tables A-1. The statistics shown were calculated using data pairs on days with observed 8-hour ozone of ≥ 60 ppb. The distributions of observed and predicted 8-hour ozone by month in the period May through September for each region are shown in Figures A-3 through A-11. Spatial plots of the mean bias and error as well as the normalized mean bias and error for individual monitors are shown in Figures A-12 through A-15. Time series plots of observed and predicted MDA 8-hour ozone during the period May through September for selected sites are provided in Figure A-16.

As indicated by the statistics in Table A-1, the base year 2016 modeling tends to under predict MDA8 ozone, although the bias and error are relatively low in each region. Generally, mean bias for 8-hour ozone ≥ 60 ppb during the period May through September is close to or within ± 10 ppb[17] in nearly all of the regions. The mean error is less than 10 ppb in the Northeast, Ohio Valley, Southeast, South, and Southwest. Normalized mean bias is within 10 percent for sites in the Northeast, Southeast, and Northwest with somewhat larger under

U.S. Environmental Protection Agency, Proposal to Designate an Emissions Control Area for Nitrogen Oxides, Sulfur Oxides, and Particulate Matter: Technical Support Document. EPA-420-R-007, 329pp., 2009. (http://www.epa.gov/otaq/regs/nonroad/marine/ci/420r09007.pdf)
Phillips, S., K. Wang, C. Jang, N. Possiel, M. Strum, T. Fox, 2007. Evaluation of 2002 Multi-pollutant Platform: Air Toxics, Ozone, and Particulate Matter, 7th Annual CMAS Conference, Chapel Hill, NC, October 6-8, 2008. (http://www.cmascenter.org/conference/2008/agenda.cfm).
U.S. Environmental Protection Agency, 2010, Renewable Fuel Standard Program (RFS2) Regulatory Impact Analysis. EPA-420-R-10-006. February 2010. Sections 3.4.2.1.2 and 3.4.3.3. Docket EPA-HQ-OAR-2009-0472-11332. (http://www.epa.gov/oms/renewablefuels/420r10006.pdf)
Simon, H., Baker, K.R., and Phillips, S. (2012) Compilation and interpretation of photochemical model performance statistics published between 2006 and 2012. *Atmospheric Environment* **61**, 124-139.

[17] Note that "within ± 10 ppb" includes values that are greater than or equal to -10 ppb and less than or equal to 10 ppb.

prediction in the other regions where the normalized mean bias is less than 15 percent. The exceptions are the Upper Midwest and the Northern Rockies where normalized mean bias is -19 percent. The normalized mean error is less than approximately 15 percent for the Northeast, Ohio Valley, Southeast, South, and Southwest and less that 20 percent in the other regions.

The monthly distributions of MDA8 model-predicted ozone for each region are provided in Figures A-3 through A-11. In the Northeast and Ohio Valley the model under predicts in May and June followed by over prediction in the remainder of the ozone season. In the Upper Midwest, the distribution of observed concentrations is under predicted in May and June, but the median and interquartile range of the model aligns with the observed data. Observed peak values in this region are notably under predicted in May, June, and August. In the Southeast, the distribution of predictions generally corresponds well with that of the observed concentrations in May and June with over prediction during the remainder of the ozone season. The distribution of predicted concentrations tends to be close to that of the observed data at the 25th percentile, median and 75th percentile values in the South with a tendency for under-prediction of peak values in May and June. In the Southwest, the modeled values align with the median and interquartile range of the observed values in May and June, but the decline in observed concentrations after June is not as notable in the model. The model under predicts in May, June, and July in the Northern Rockies but closely captures the distribution of observed concentrations in August and September. In the Northwest modeled MDA8 ozone under predicts in May and June, but then closely tracks the observed values in July, August, and September. The median and interquartile range of observed ozone is under predicted in May through September in the West region.

Figures A-12 through A-15 show the spatial variability in bias and error at monitor locations for MDA8 ozone on days with measured concentrations $\geq$ 60 ppb. Mean bias, as seen from Figure A-12, is within $\pm$ 5 ppb at many sites from portions of Texas northeastward to the Northeast Corridor. In this area, the normalized mean bias is within $\pm$ 10 percent, the mean error is mainly less than 10 ppb and the normalized mean error is between 5 to 15 percent. At most monitoring sites across the remainder of the East the model under predicts by 5 to 10 ppb, the normalized mean bias is between -10 and -20 percent, the mean error is in the range of 10 to 15 ppb, with normalized mean error of 10 to 15 percent. The exceptions are at some monitoring

sites mainly in the interior parts of Michigan, Wisconsin, the northern portions of Indiana and Illinois, and Upstate New York where the magnitude of under prediction is 10 to 15 ppb, the normalized mean bias is -10 to -30 percent, the mean error is 10 to 15 ppb, and the normalized mean error is 15 to 25 percent. Elsewhere in the U.S., there is notable heterogeneity in mean bias. For example, there are sites with mean bias showing under prediction of 5 to 10 ppb while at other sites in the same area the model under prediction is 10 to 15 ppb. Similar heterogeneity is evident in other performance metrics.

In addition to the above analysis of overall model performance, we also examine how well the modeling platform replicates day to day fluctuations in observed 8-hour daily maximum concentrations for selected monitoring sites. For this site-specific analysis we present the time series of observed and predicted 8-hour daily maximum concentrations by site over the period May through September. The results, as shown in Figures A-16, indicate that the modeling platform generally replicates the day-to-day variability in ozone during this time period at these sites. That is, days with high modeled concentrations are generally also days with high measured concentrations and, conversely, days with low modeled concentrations are also days with low measured concentrations in most cases. Model predictions at these sites not only accurately capture the day-to-day variability in the observations, but also appear to capture the timing and general magnitude of multi-day high ozone episodes as well as time periods of relatively low concentrations. However, there is a tendency for under prediction of peak MDA8 concentrations at certain sites during specific episodes.

In summary, the ozone model performance statistics for the CAMx 2016fj (2016v2) simulation are within or close to the ranges found in other recent peer-reviewed applications (e.g., Simon et al, 2012 and Emory et al, 2017). As described in this appendix, the predictions from the 2016v2 modeling platform correspond closely to observed concentrations in terms of the magnitude, temporal fluctuations, and geographic differences for 8-hour daily maximum ozone. Thus, the model performance results demonstrate the scientific credibility of our 2016v2 modeling platform. These results provide confidence in the ability of the modeling platform to provide a reasonable projection of expected future year ozone concentrations and contributions.

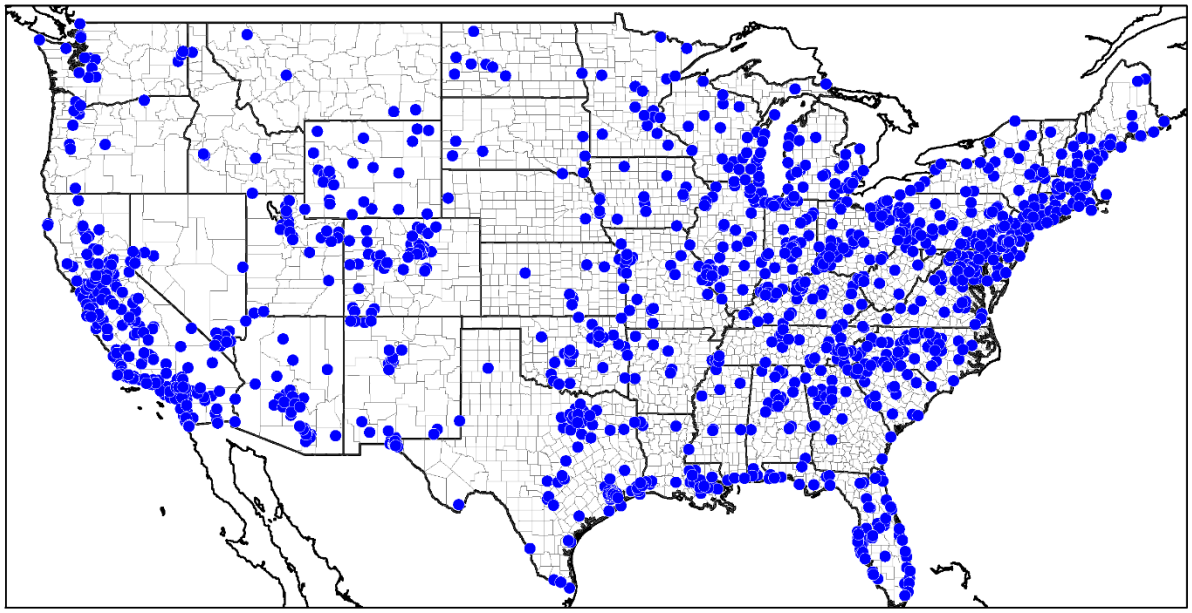

Figure A-1a. Location of ozone monitoring sites.

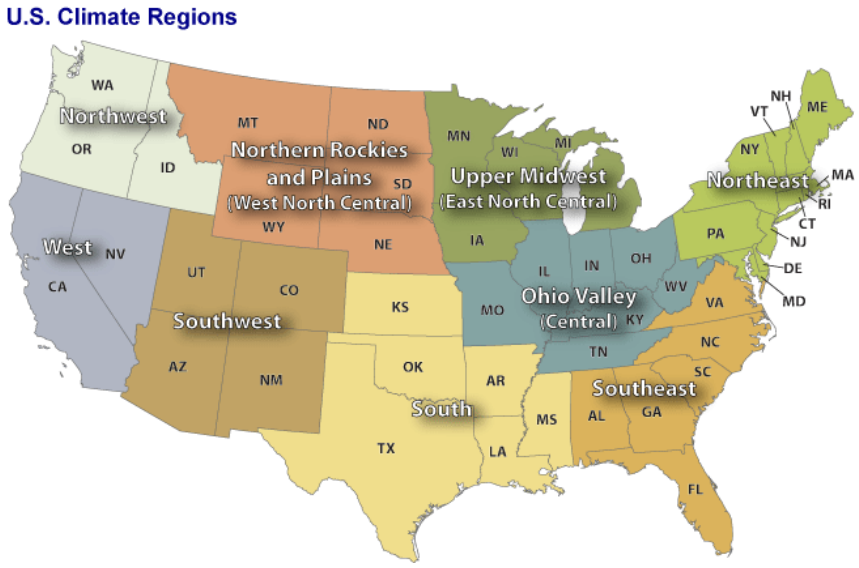

Figure A-2. NOAA climate regions (source: http://www.ncdc.noaa.gov/monitoring-references/maps/us-climate-regions.php#references)

Table A-1. Performance statistics for MDA8 ozone ≥ 60 ppb for May through September by climate region.

Climate Region	Number of Days ≥ 60 ppb	MB (ppb)	ME (ppb)	NMB (%)	NME (%)
Northeast	2997	-4.1	7.1	-6.2	10.7
Ohio Valley	3211	-7.1	8.7	-10.9	13.3
Upper Midwest	1134	-12.7	13.0	-19.1	19.5
Southeast	1477	-2.9	6.1	-4.5	9.4
South	993	-7.8	9.1	-12.0	14.1
Southwest	3054	-8.8	9.7	-13.6	15.1
Northern Rockies	215	-11.9	12.4	-19.0	19.8
Northwest	84	-5.8	10.8	-9.0	16.6
West	8279	-9.7	11.4	-13.8	16.2

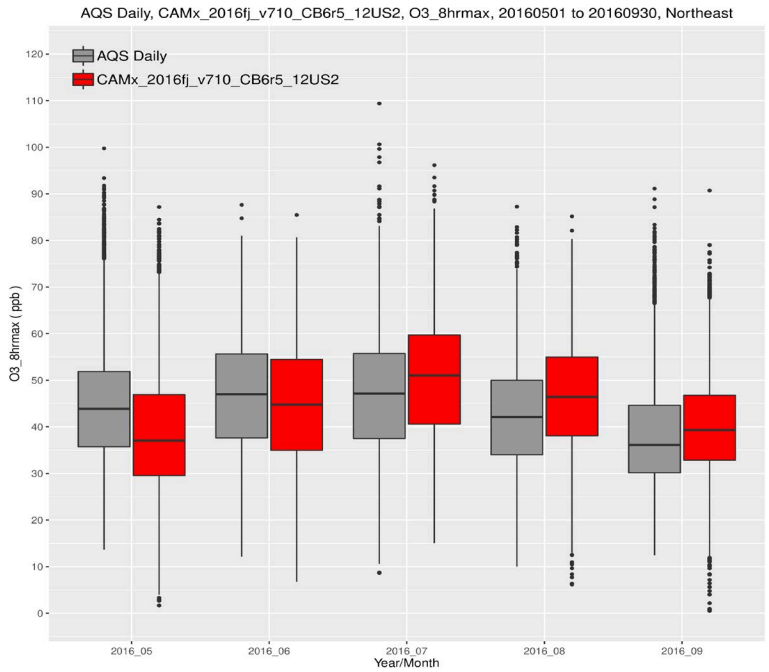

Figure A-3. Distribution of observed and predicted MDA8 ozone by month for the period May through September for the Northeast region, [line within box = median; top/bottom of box = 75th/25th percentiles; top/bottom dots = peak/minimum values]

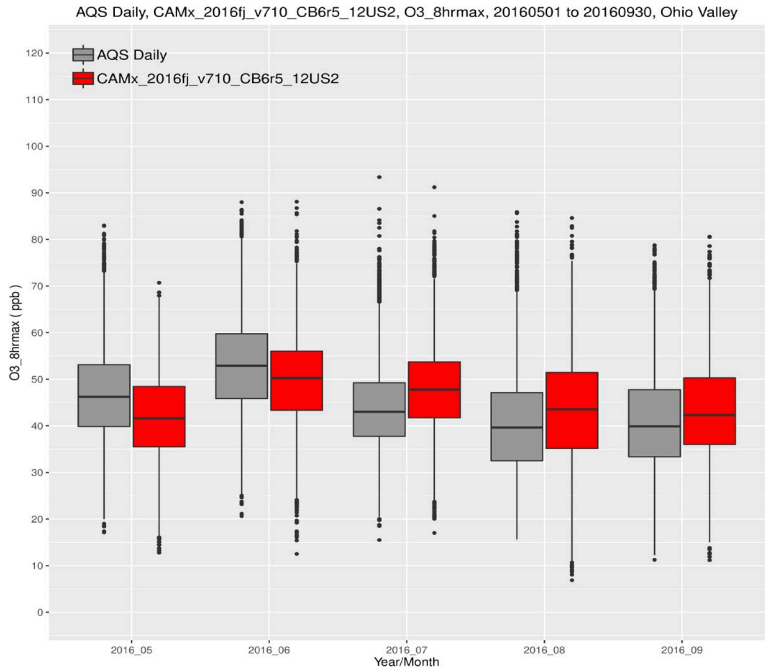

Figure A-4. Distribution of observed and predicted MDA8 ozone by month for the period May through September for the Ohio Valley region.

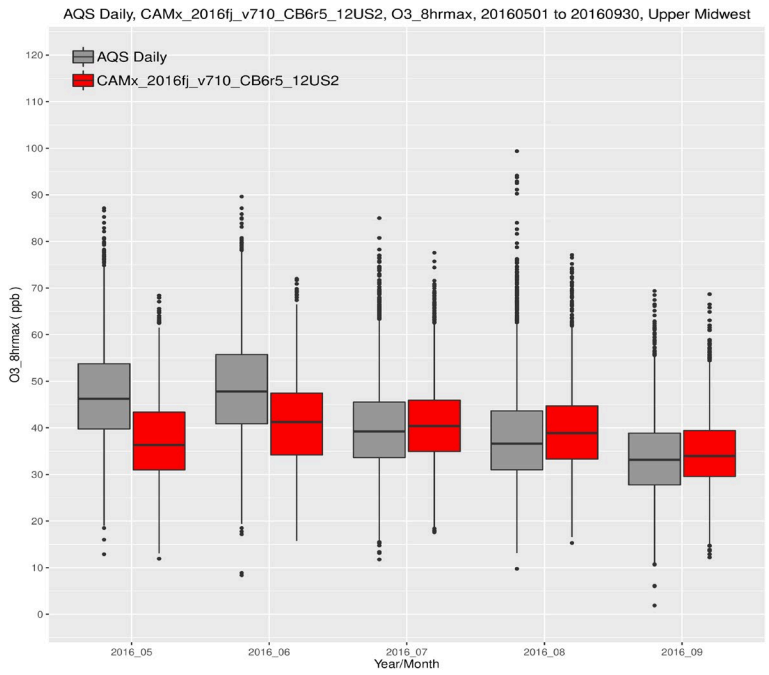

Figure A-5. Distribution of observed and predicted MDA8 ozone by month for the period May through September for the Upper Midwest region.

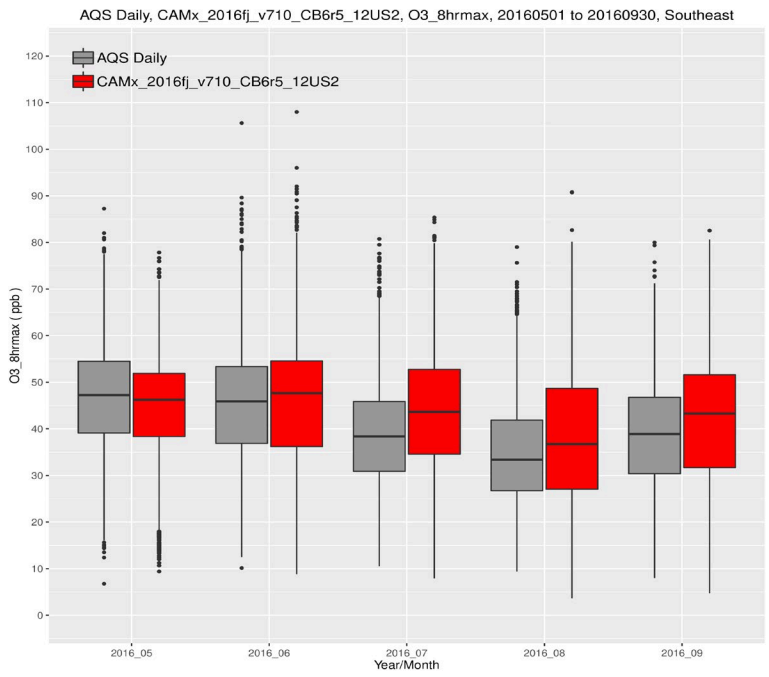

Figure A-6. Distribution of observed and predicted MDA8 ozone by month for the period May through September for the Southeast region.

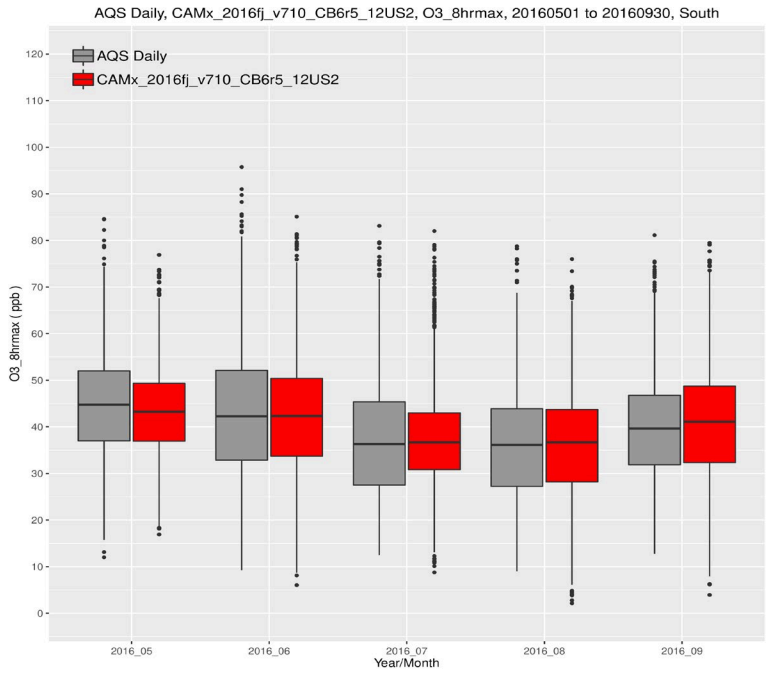

Figure A-7. Distribution of observed and predicted MDA8 ozone by month for the period May through September for the South region.

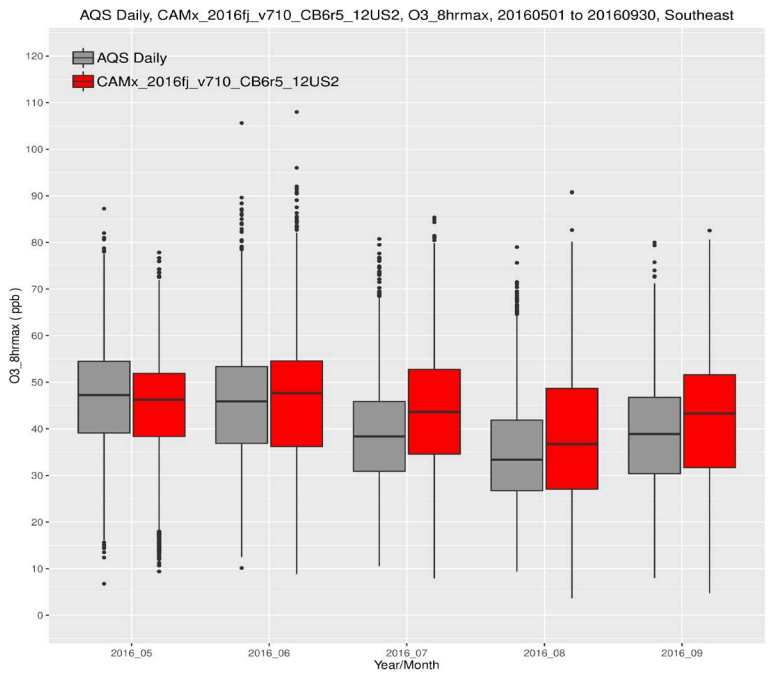

Figure A-8. Distribution of observed and predicted MDA8 ozone by month for the period May through September for the Southwest region.

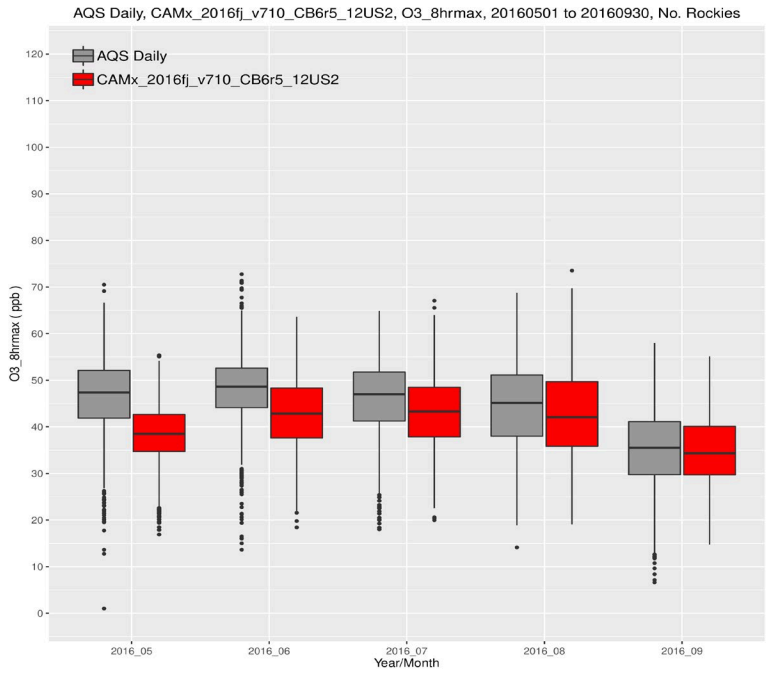

Figure A-9. Distribution of observed and predicted MDA8 ozone by month for the period May through September for the Northern Rockies region.

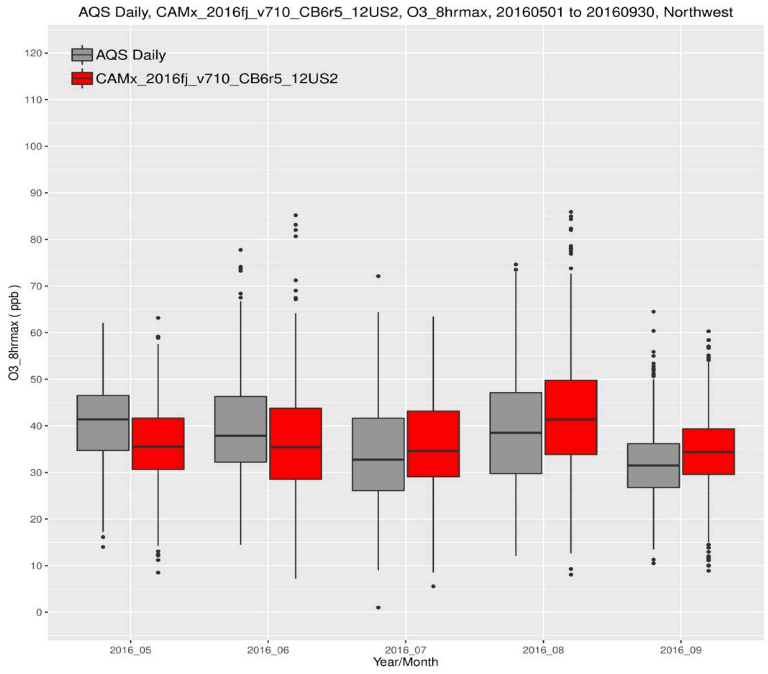

Figure A-10. Distribution of observed and predicted MDA8 ozone by month for the period May through September for the Northwest region.

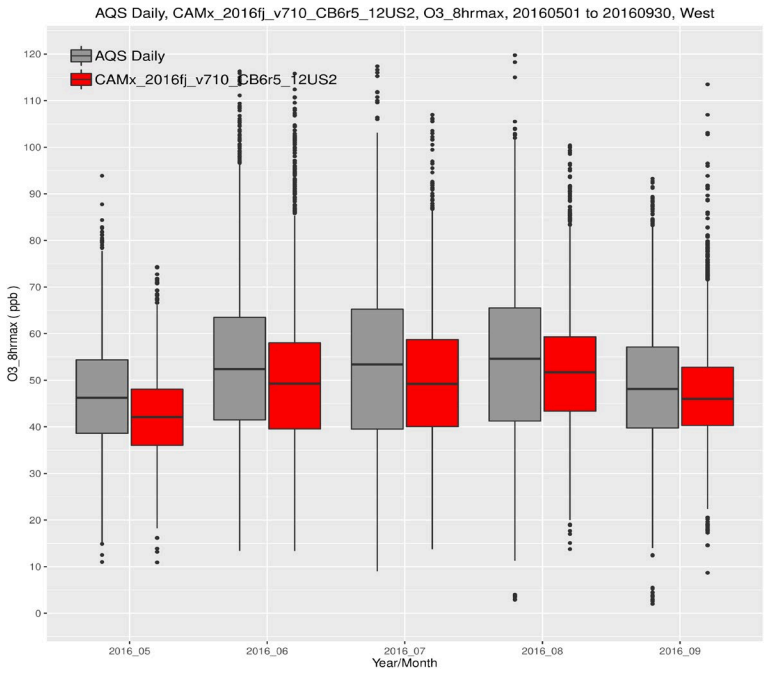

Figure A-11. Distribution of observed and predicted MDA8 ozone by month for the period May through September for the West region.

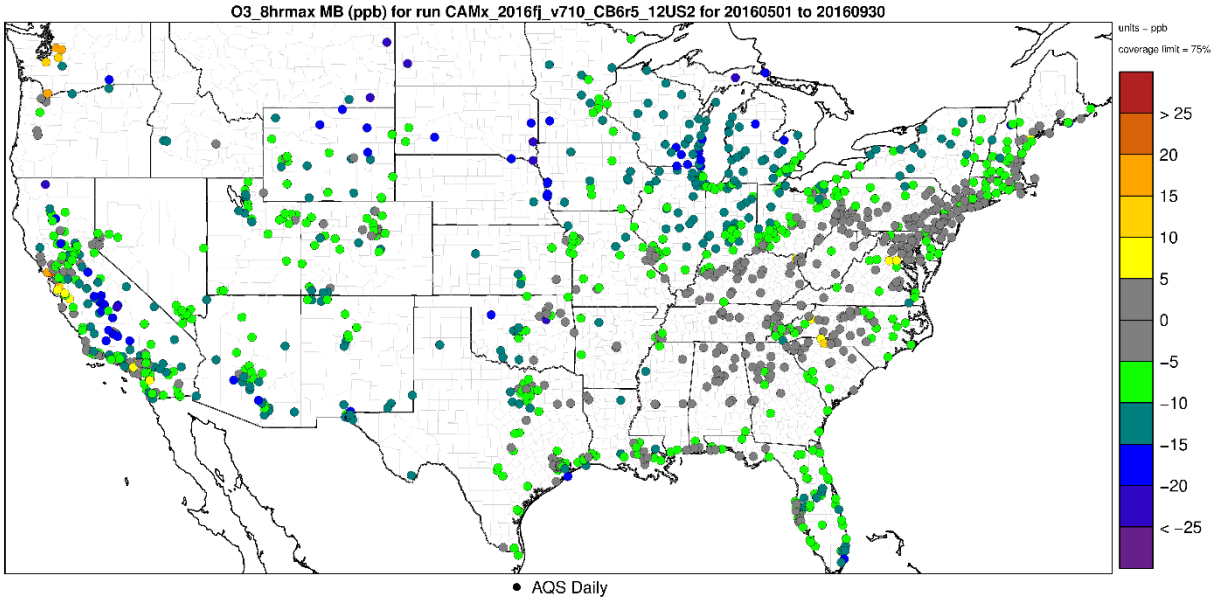

Figure A-12. Mean Bias (ppb) of MDA8 ozone ≥ 60 ppb over the period May-September, paired in time and space.

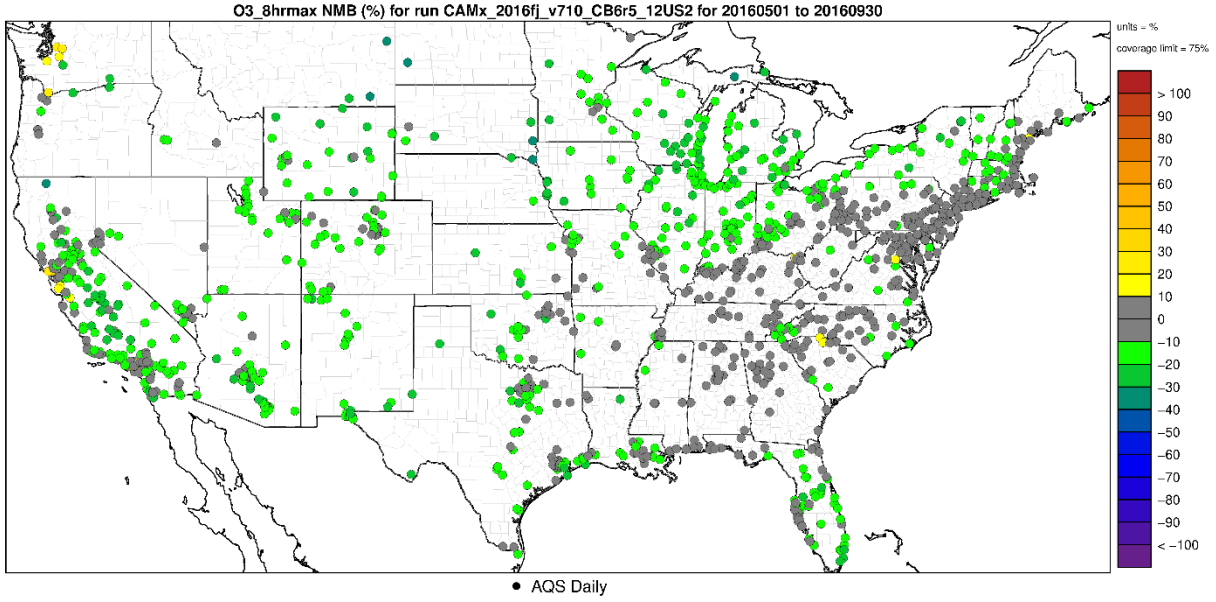

Figure A-13. Normalized Mean Bias (%) of MDA8 ozone ≥ 60 ppb over the period May-September 2016, paired in space and time.

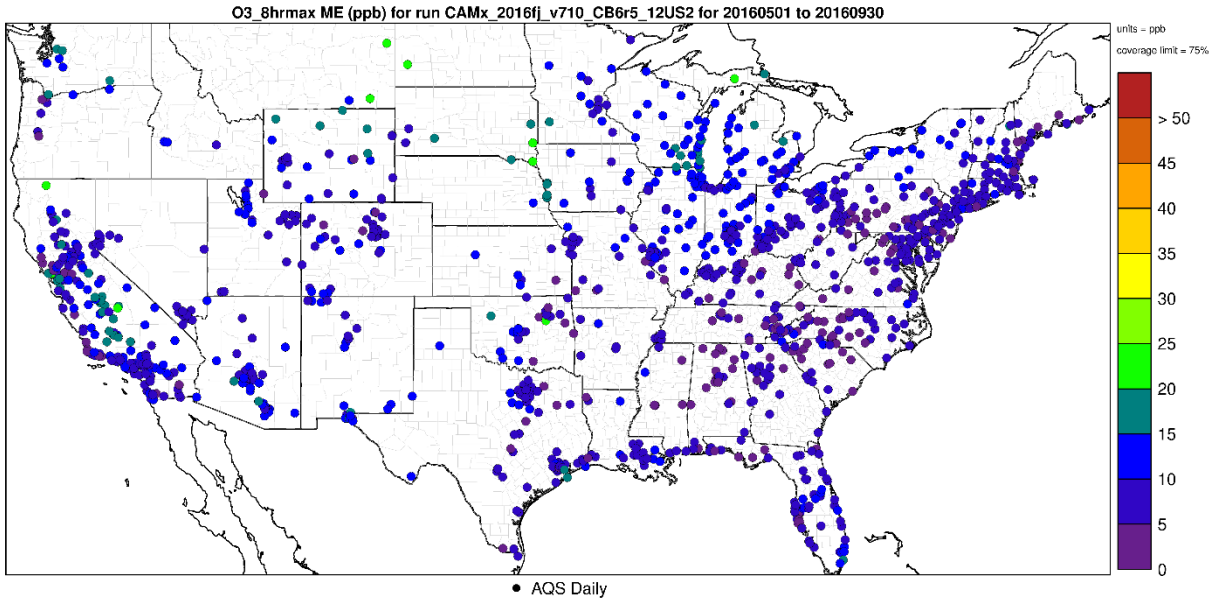

Figure A-14. Mean Error (ppb) of MDA8 ozone ≥ 60 ppb over the period May-September 2016, paired in time and space.

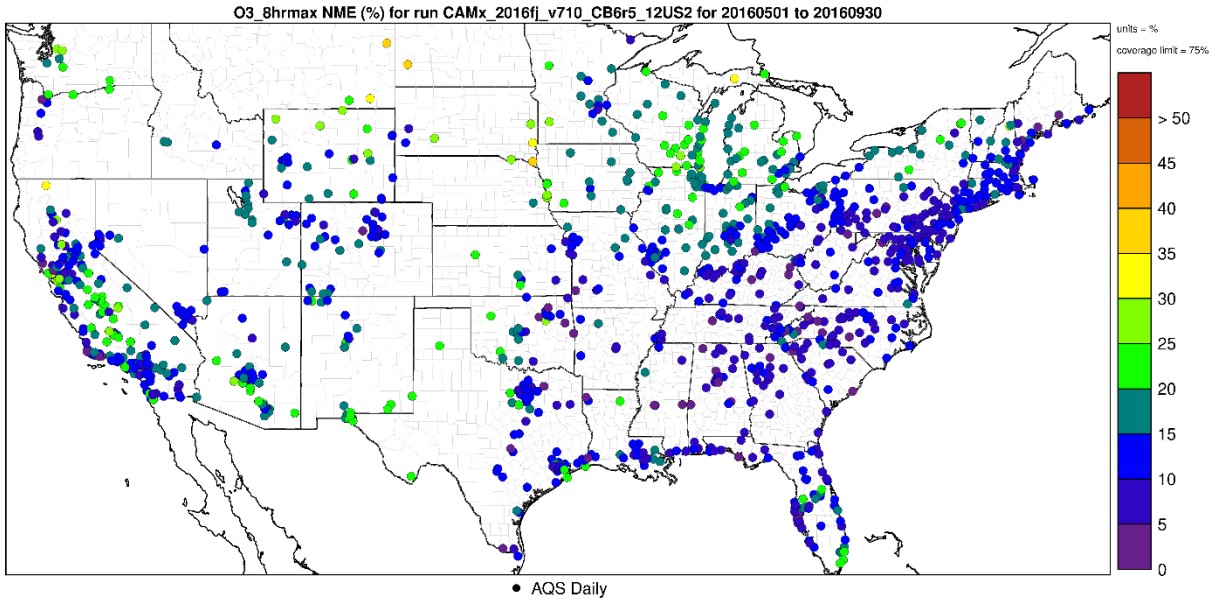

Figure A-15. Normalized Mean Error (%) of MDA8 ozone ≥ 60 ppb over the period May-September 2016, paired in time and space.

Figure A-16. Time series of observed and predicted MDA8 ozone concentrations for the period May 1 through September 30, 2016 for selected high ozone monitoring site.

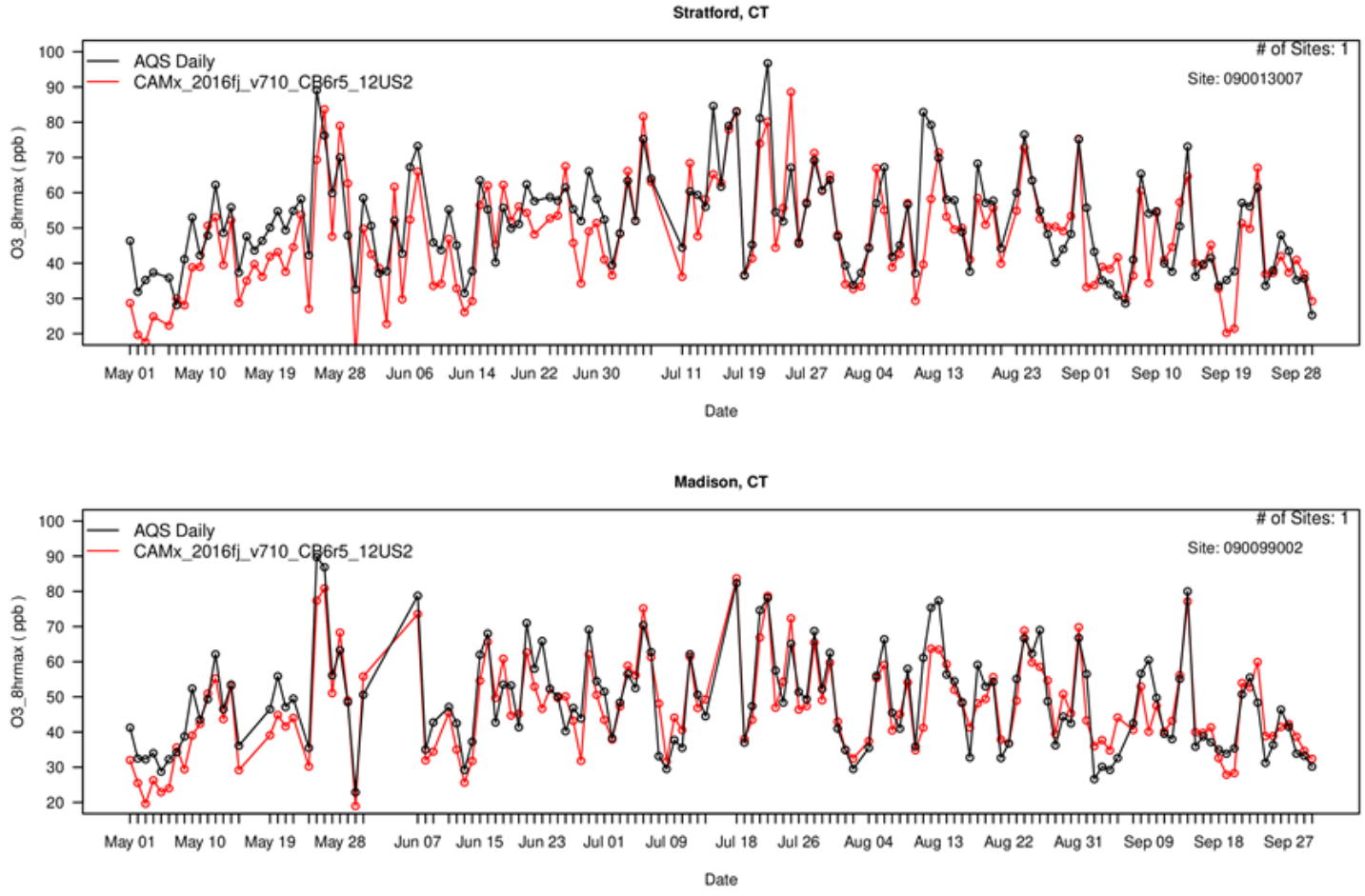

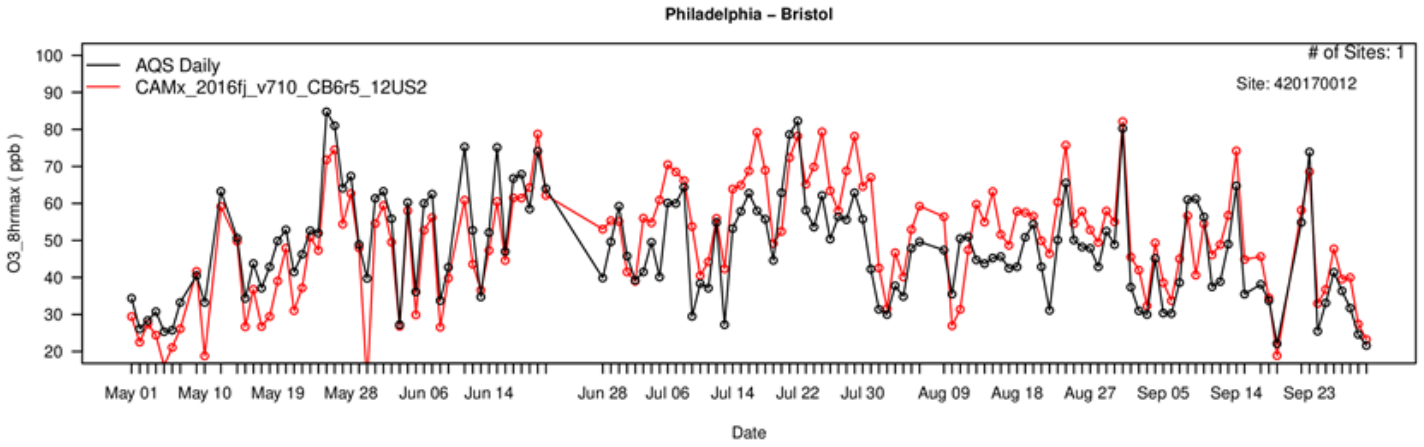
Philadelphia – Bristol
AQS Daily
CAMx_2016fj_v710_CB6r5_12US2
# of Sites: 1
Site: 420170012
O3_8hrmax (ppb)
100
90
80
70
60
50
40
30
20
May 01
May 10
May 19
May 28
Jun 06
Jun 14
Jun 28
Jul 06
Jul 14
Jul 22
Jul 30
Aug 09
Aug 18
Aug 27
Sep 05
Sep 14
Sep 23
Date

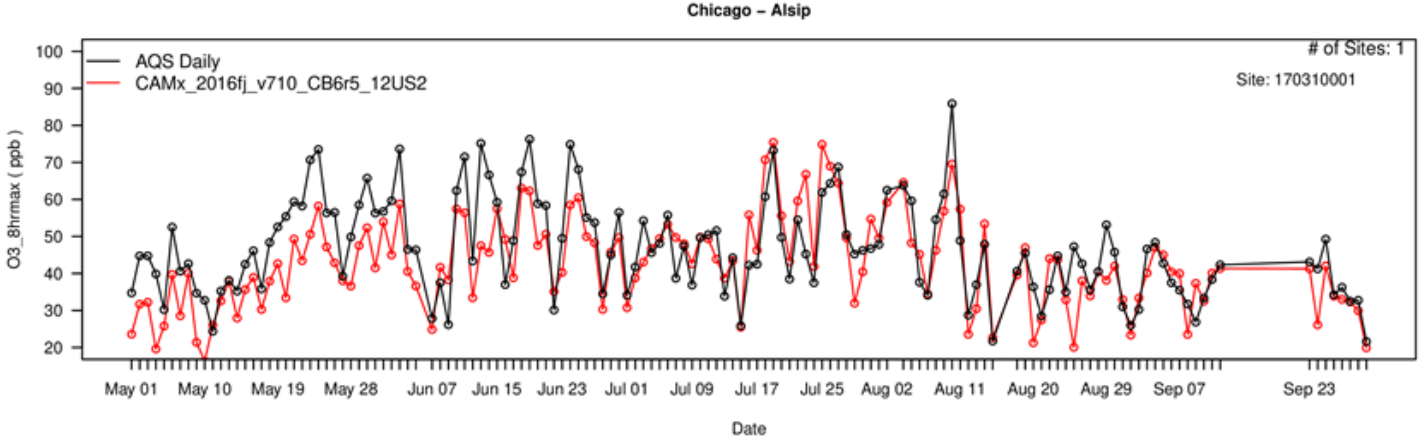
Chicago – Alsip
AQS Daily
CAMx_2016fj_v710_CB6r5_12US2
# of Sites: 1
Site: 170310001
O3_8hrmax (ppb)
100
90
80
70
60
50
40
30
20
May 01
May 10
May 19
May 28
Jun 07
Jun 15
Jun 23
Jul 01
Jul 09
Jul 17
Jul 25
Aug 02
Aug 11
Aug 20
Aug 29
Sep 07
Sep 23
Date

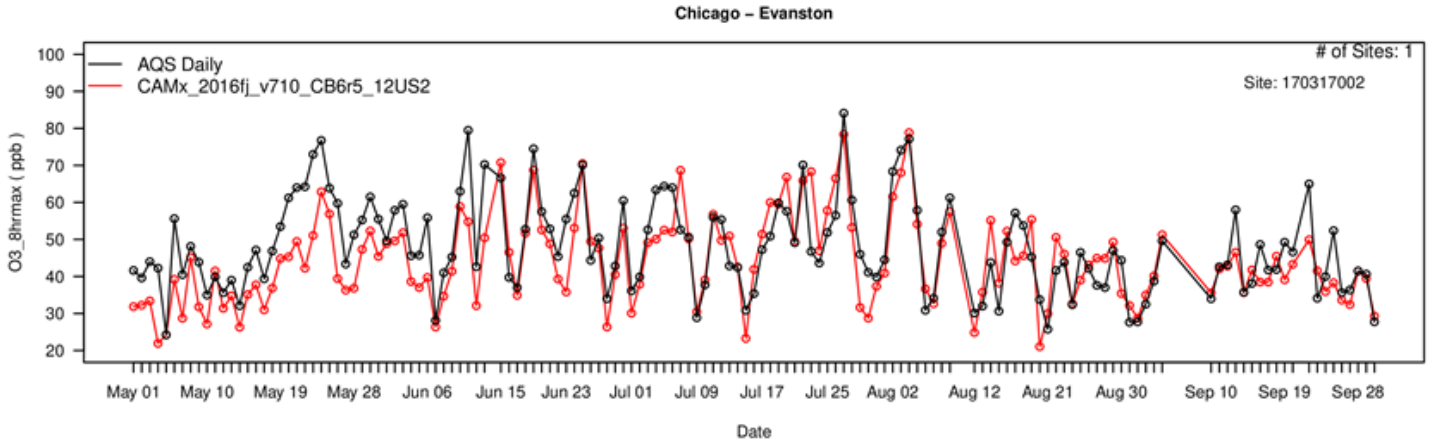
Chicago – Evanston
AQS Daily
CAMx_2016fj_v710_CB6r5_12US2
# of Sites: 1
Site: 170317002
O3_8hrmax (ppb)
100
90
80
70
60
50
40
30
20
May 01
May 10
May 19
May 28
Jun 06
Jun 15
Jun 23
Jul 01
Jul 09
Jul 17
Jul 25
Aug 02
Aug 12
Aug 21
Aug 30
Sep 10
Sep 19
Sep 28
Date

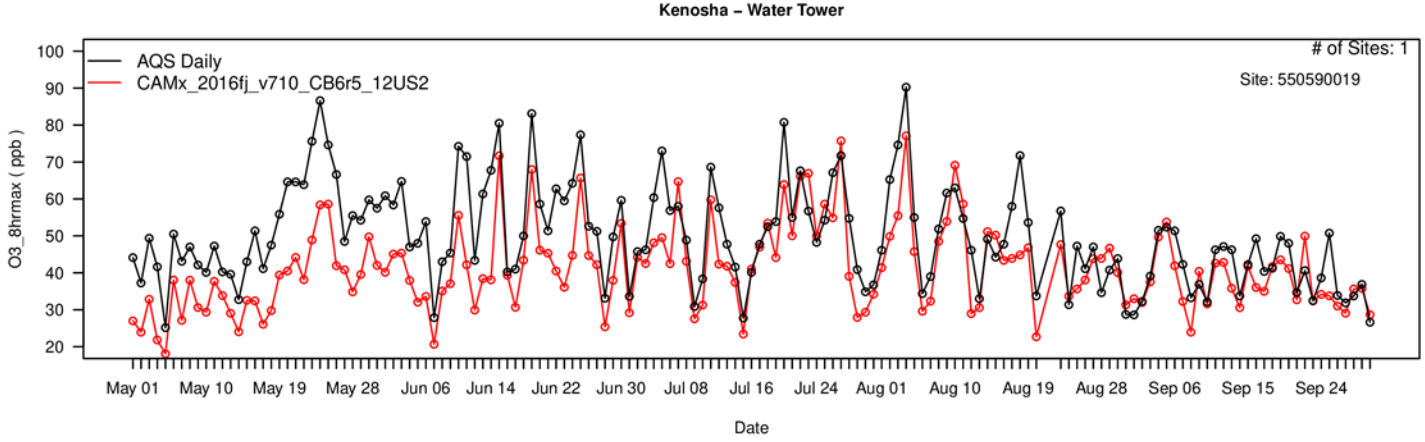
Kenosha – Water Tower
AQS Daily
CAMx_2016fj_v710_CB6r5_12US2
# of Sites: 1
Site: 550590019
O3_8hrmax (ppb)
100
90
80
70
60
50
40
30
20
May 01
May 10
May 19
May 28
Jun 06
Jun 14
Jun 22
Jun 30
Jul 08
Jul 16
Jul 24
Aug 01
Aug 10
Aug 19
Aug 28
Sep 06
Sep 15
Sep 24
Date

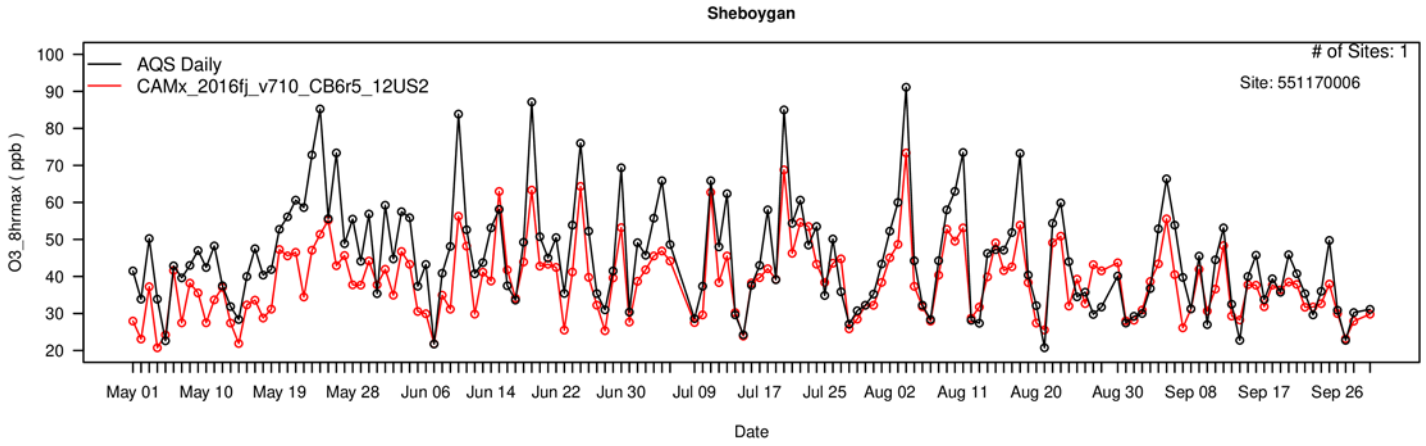
Sheboygan
AQS Daily
CAMx_2016fj_v710_CB6r5_12US2
# of Sites: 1
Site: 551170006
O3_8hrmax (ppb)
100
90
80
70
60
50
40
30
20
May 01
May 10
May 19
May 28
Jun 06
Jun 14
Jun 22
Jun 30
Jul 09
Jul 17
Jul 25
Aug 02
Aug 11
Aug 20
Aug 30
Sep 08
Sep 17
Sep 26
Date

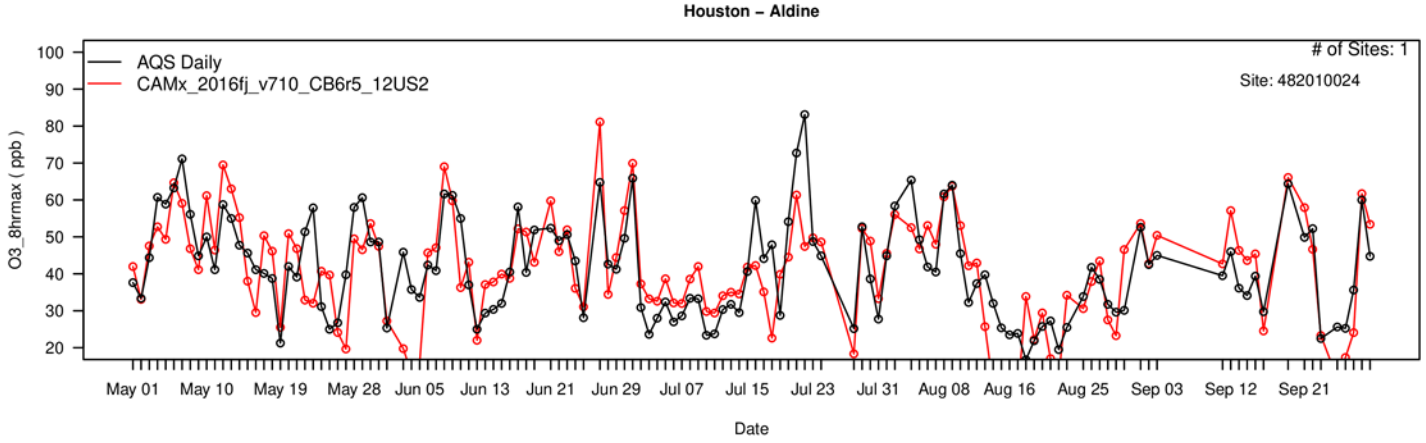
Houston – Aldine
AQS Daily
CAMx_2016fj_v710_CB6r5_12US2
# of Sites: 1
Site: 482010024
O3_8hrmax (ppb)
100
90
80
70
60
50
40
30
20
May 01
May 10
May 19
May 28
Jun 05
Jun 13
Jun 21
Jun 29
Jul 07
Jul 15
Jul 23
Jul 31
Aug 08
Aug 16
Aug 25
Sep 03
Sep 12
Sep 21
Date

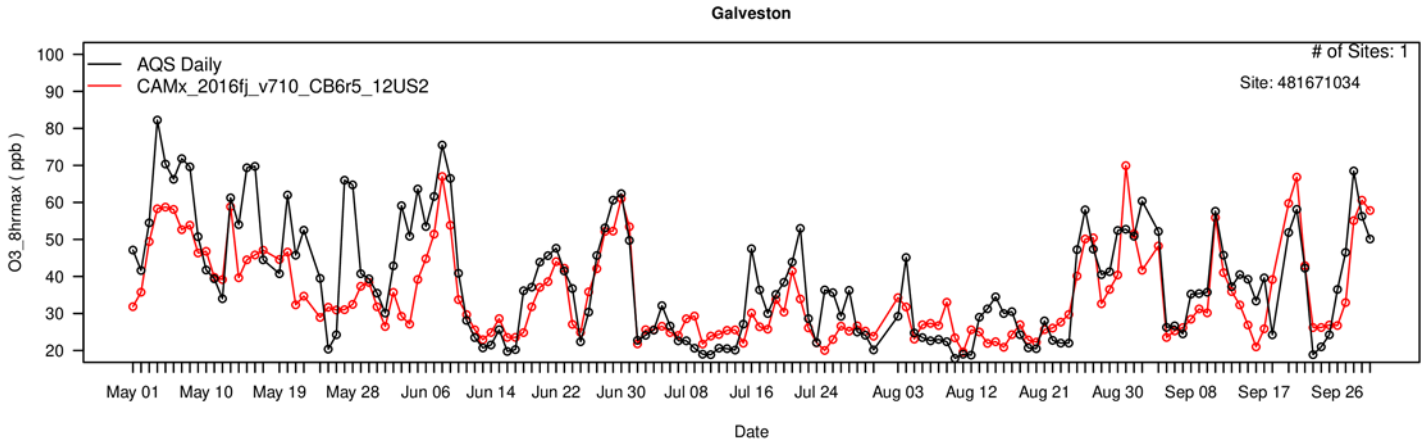
Galveston
AQS Daily
CAMx_2016fj_v710_CB6r5_12US2
# of Sites: 1
Site: 481671034
O3_8hrmax (ppb)
100
90
80
70
60
50
40
30
20
May 01
May 10
May 19
May 28
Jun 06
Jun 14
Jun 22
Jun 30
Jul 08
Jul 16
Jul 24
Aug 03
Aug 12
Aug 21
Aug 30
Sep 08
Sep 17
Sep 26
Date

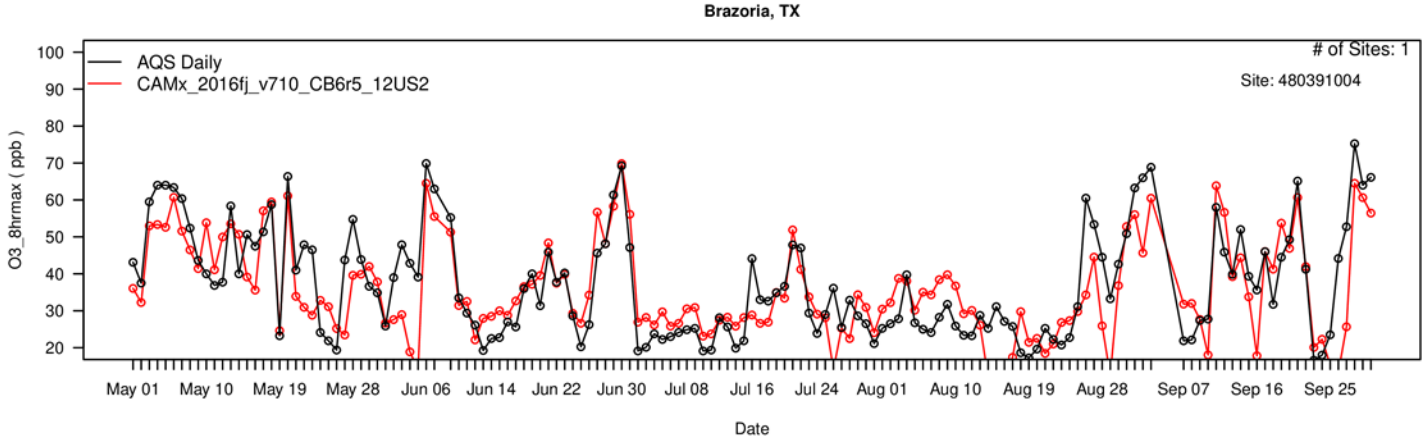
Brazoria, TX
AQS Daily
CAMx_2016fj_v710_CB6r5_12US2
# of Sites: 1
Site: 480391004
O3_8hrmax (ppb)
100
90
80
70
60
50
40
30
20
May 01
May 10
May 19
May 28
Jun 06
Jun 14
Jun 22
Jun 30
Jul 08
Jul 16
Jul 24
Aug 01
Aug 10
Aug 19
Aug 28
Sep 07
Sep 16
Sep 25
Date

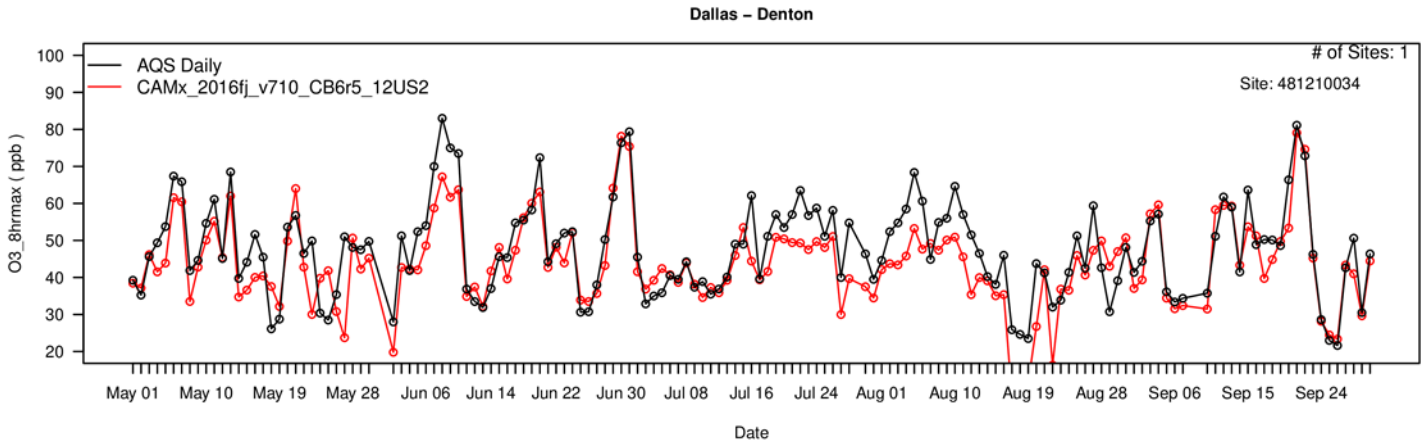
Dallas – Denton
AQS Daily
CAMx_2016fj_v710_CB6r5_12US2
# of Sites: 1
Site: 481210034
O3_8hrmax (ppb)
100
90
80
70
60
50
40
30
20
May 01
May 10
May 19
May 28
Jun 06
Jun 14
Jun 22
Jun 30
Jul 08
Jul 16
Jul 24
Aug 01
Aug 10
Aug 19
Aug 28
Sep 06
Sep 15
Sep 24
Date

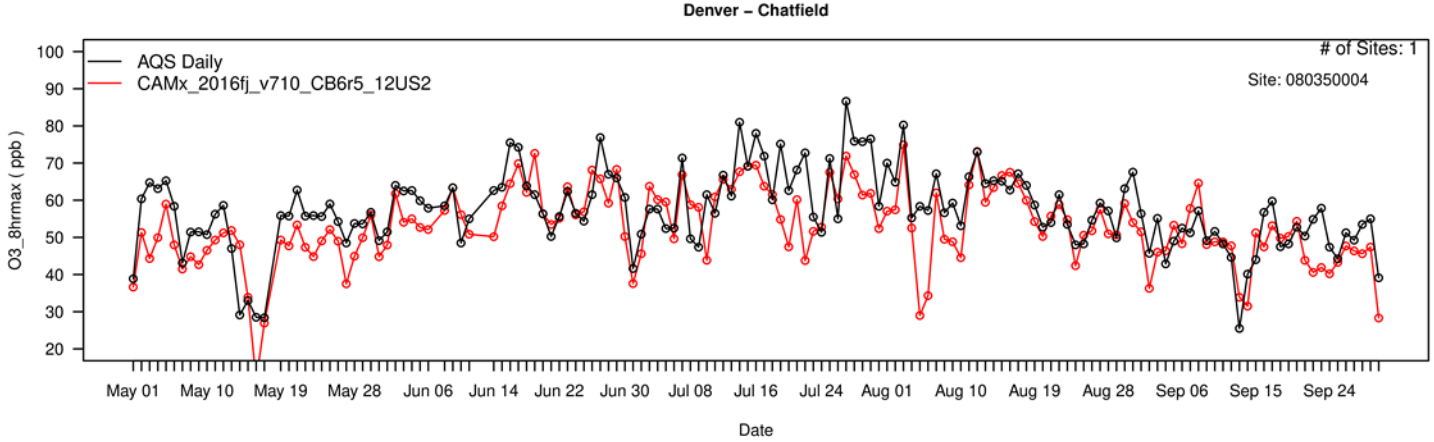
Denver – Chatfield
AQS Daily
CAMx_2016fj_v710_CB6r5_12US2
# of Sites: 1
Site: 080350004
O3_8hrmax (ppb)
100
90
80
70
60
50
40
30
20
May 01
May 10
May 19
May 28
Jun 06
Jun 14
Jun 22
Jun 30
Jul 08
Jul 16
Jul 24
Aug 01
Aug 10
Aug 19
Aug 28
Sep 06
Sep 15
Sep 24
Date

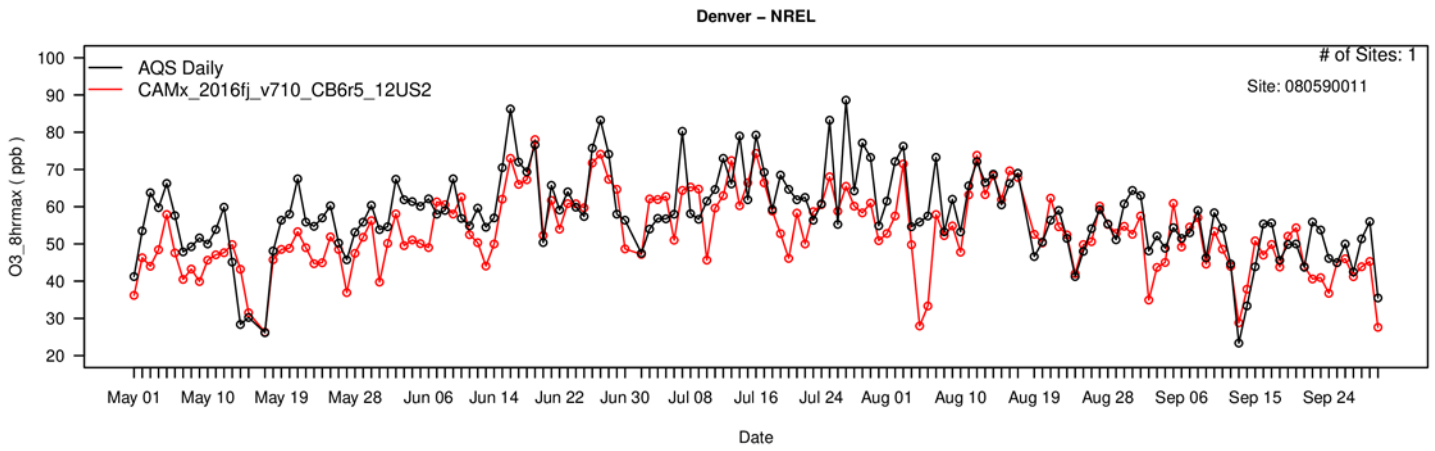
Denver – NREL
AQS Daily
CAMx_2016fj_v710_CB6r5_12US2
# of Sites: 1
Site: 080590011
O3_8hrmax (ppb)
100
90
80
70
60
50
40
30
20
May 01
May 10
May 19
May 28
Jun 06
Jun 14
Jun 22
Jun 30
Jul 08
Jul 16
Jul 24
Aug 01
Aug 10
Aug 19
Aug 28
Sep 06
Sep 15
Sep 24
Date

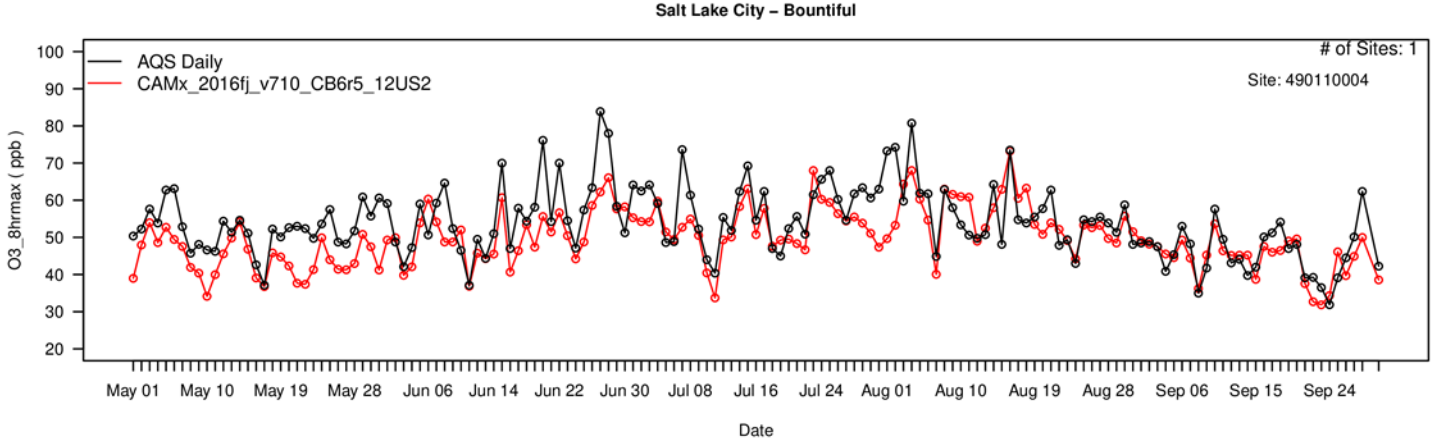
Salt Lake City – Bountiful
AQS Daily
CAMx_2016fj_v710_CB6r5_12US2
# of Sites: 1
Site: 490110004
O3_8hrmax (ppb)
100
90
80
70
60
50
40
30
20
May 01
May 10
May 19
May 28
Jun 06
Jun 14
Jun 22
Jun 30
Jul 08
Jul 16
Jul 24
Aug 01
Aug 10
Aug 19
Aug 28
Sep 06
Sep 15
Sep 24
Date

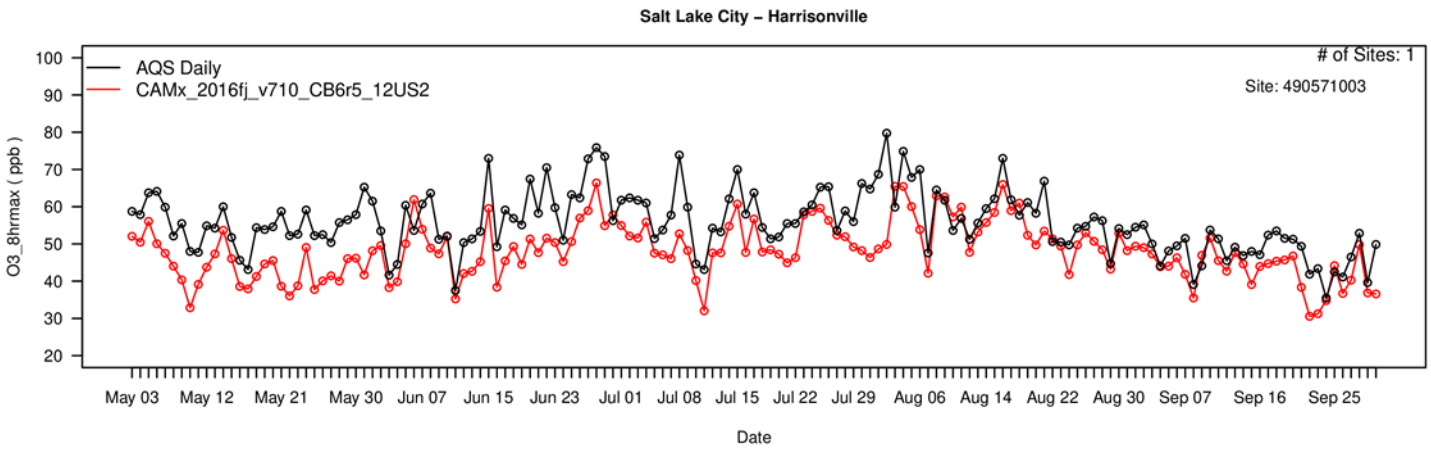
Salt Lake City – Harrisonville
AQS Daily
CAMx_2016fj_v710_CB6r5_12US2
# of Sites: 1
Site: 490571003
O3_8hrmax (ppb)
100
90
80
70
60
50
40
30
20
May 03
May 12
May 21
May 30
Jun 07
Jun 15
Jun 23
Jul 01
Jul 08
Jul 15
Jul 22
Jul 29
Aug 06
Aug 14
Aug 22
Aug 30
Sep 07
Sep 16
Sep 25
Date

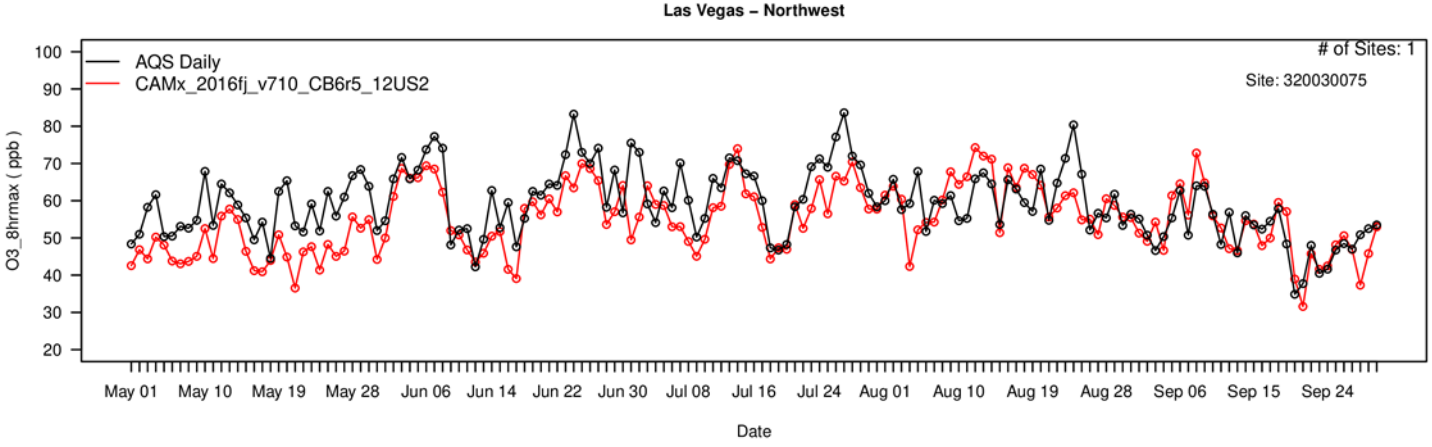
Las Vegas – Northwest
AQS Daily
CAMx_2016fj_v710_CB6r5_12US2
# of Sites: 1
Site: 320030075
O3_8hrmax (ppb)
100
90
80
70
60
50
40
30
20
May 01
May 10
May 19
May 28
Jun 06
Jun 14
Jun 22
Jun 30
Jul 08
Jul 16
Jul 24
Aug 01
Aug 10
Aug 19
Aug 28
Sep 06
Sep 15
Sep 24
Date

Appendix G-2
EPA 2016v2 DVs
Summary

README FILE

This file contains base period and projected ozone design values and projected contributions at individual monitoring sites based upon EPA's air quality modeling for the 2016v2 Emissions Modeling Platform.

The following data are provided for individual monitoring sites:

- 2023, 2026, and 2032 average and maximum design values for the "3 x 3" and "no water" approaches.
- Measured 2014 - 2018 average and maximum design values (i.e., 2016-Centered Avg and Max DVs).
- 2020 Measured design values.
- 2023 and 2026 ozone contribution metric values from each state and the District of Columbia, individually.
- 2023 and 2026 ozone contribution metric values from emissions in the Tribal, Canada & Mexico, Offshore, Fires, Initial & Boundary Concentration, and Biogenics source tags.

Notes:

- The concentrations and contribution data in this file are in units of parts per billion (ppb).
- The contribution metric data for 2023 and 2026 are based on apportioning the 2023 and 2026 "no water" average design values using the modeled contribution data for each of these years, respectively.
- Data in this file are provided for those monitoring sites that meet certain criteria used for calculating the contribution metric. Specifically, the contribution metric values are calculated based on modeled contribution data for the top-10 model-predicted 8-hour daily maximum (i.e., MDA8) ozone concentration days in the future year modeling. Monitoring sites were eliminated from the calculation of the contribution metric if there were fewer than 5 days with future year modeled-predicted MDA8 ozone concentrations greater than or equal to 60 ppb. Note that the calculation of contribution metric values for 2026 are based on daily contributions for the same set of days used to calculated the contribution metric values for 2023 at each monitoring site.
- Additional information on the methods for projecting design values and calculating contributions can be found in the Air Quality Modeling for the 2016v2 Emissions Platform Technical Support Document.
- Design values at monitoring sites with measured exceedance that are primarily associated certain wintertime meteorological conditions and ozone precursor emissions from oil and gas production and transportation have been excluded from this data set. This includes the monitoring sites in Duchesne and Uintah counties, UT.

2023_2026_2032_DVs_3x3

Site ID	State	County	2016-Centered Avg	2016-Centered Max	2023fj Avg 3x3	2023fj Max 3x3	2026fj Avg 3x3	2026fj Max 3x3	2032fj Avg 3x3	2032fj Max 3x3
240031003	Maryland	Anne Arundel	74.0	74	64.7	64.7	63.0	63.0	61.3	61.3
240051007	Maryland	Baltimore	72.0	72	62.3	62.3	60.6	60.6	58.9	58.9
240053001	Maryland	Baltimore	72.7	73	63.7	63.9	62.0	62.3	60.4	60.6
240090011	Maryland	Calvert	67.7	69	58.6	59.7	57.0	58.1	55.4	56.4
240130001	Maryland	Carroll	68.3	69	58.9	59.5	57.3	57.9	55.6	56.2
240150003	Maryland	Cecil	74.0	74	63.4	63.4	61.7	61.7	60.0	60.0
240170010	Maryland	Charles	69.3	70	59.5	60.1	57.7	58.3	55.8	56.4
240190004	Maryland	Dorchester	64.7	66	56.2	57.3	54.6	55.7	53.0	54.1
240199991	Maryland	Dorchester	65.7	66	57.1	57.4	55.5	55.8	54.1	54.3
240210037	Maryland	Frederick	68.0	69	58.4	59.3	56.9	57.7	55.2	56.0
240230002	Maryland	Garrett	65.3	66	57.4	58.0	54.5	55.1	53.3	53.9
240251001	Maryland	Harford	74.0	75	64.4	65.3	62.7	63.5	61.0	61.8
240259001	Maryland	Harford	73.0	73	62.9	62.9	61.2	61.2	59.5	59.5
240290002	Maryland	Kent	69.3	70	59.6	60.2	58.1	58.7	56.6	57.2
240313001	Maryland	Montgomery	67.7	68	59.0	59.2	57.4	57.6	55.6	55.8
240330030	Maryland	Prince George's	69.3	70	60.5	61.1	58.8	59.4	57.0	57.6
240338003	Maryland	Prince George's	70.7	71	61.7	62.0	59.9	60.2	58.1	58.3
240339991	Maryland	Prince George's	69.3	71	60.2	61.7	58.5	59.9	56.7	58.1
240430009	Maryland	Washington	66.7	67	58.2	58.4	56.6	56.9	55.1	55.3
245100054	Maryland	Baltimore (City)	68.3	70	60.0	61.5	58.5	59.9	56.9	58.3

2023_2026_2032_DVs_3x3_No Water

Site ID	State	County	2016-Centered Avg	2016-Centered Max	2023fj Avg No Water	2023fj Max No Water	2026fj Avg No Water	2026fj Max No Water	2032fj Avg No Water	2032fj Max No Water
240031003	Maryland	Anne Arundel	74.0	74	64.4	64.4	62.6	62.6	60.8	60.8
240051007	Maryland	Baltimore	72.0	72	62.3	62.3	60.6	60.6	58.9	58.9
240053001	Maryland	Baltimore	72.7	73	62.9	63.2	61.3	61.5	59.6	59.9
240090011	Maryland	Calvert	67.7	69	57.0	58.1	55.1	56.2	53.4	54.4
240130001	Maryland	Carroll	68.3	69	58.9	59.5	57.3	57.9	55.6	56.2
240150003	Maryland	Cecil	74.0	74	63.4	63.4	61.7	61.7	60.0	60.0
240170010	Maryland	Charles	69.3	70	59.5	60.1	57.7	58.3	55.8	56.4
240190004	Maryland	Dorchester	64.7	66	55.9	57.1	54.3	55.4	52.8	53.8
240199991	Maryland	Dorchester	65.7	66	55.8	56.1	54.2	54.4	52.6	52.8
240210037	Maryland	Frederick	68.0	69	58.4	59.3	56.9	57.7	55.2	56.0
240230002	Maryland	Garrett	65.3	66	57.4	58.0	54.5	55.1	53.3	53.9
240251001	Maryland	Harford	74.0	75	63.9	64.8	62.3	63.1	60.6	61.4
240259001	Maryland	Harford	73.0	73	62.9	62.9	61.2	61.2	59.5	59.5
240290002	Maryland	Kent	69.3	70	59.6	60.2	58.1	58.7	56.6	57.2
240313001	Maryland	Montgomery	67.7	68	59.0	59.2	57.4	57.6	55.6	55.8
240330030	Maryland	Prince George's	69.3	70	60.5	61.1	58.8	59.4	57.0	57.6
240338003	Maryland	Prince George's	70.7	71	61.7	62.0	59.9	60.2	58.1	58.3
240339991	Maryland	Prince George's	69.3	71	60.2	61.7	58.5	59.9	56.7	58.1
240430009	Maryland	Washington	66.7	67	58.2	58.4	56.6	56.9	55.1	55.3
245100054	Maryland	Baltimore (City)	68.3	70	59.1	60.6	57.5	59.0	56.0	57.4